Article:

Shiers, MN, Hodgson, DM orcid.org/0000-0003-3711-635X and Mountney, NP orcid.org/0000-0002-8356-9889 (2017) Response of a Coal-Bearing Coastal Plain Succession to Marine Transgression: Campanian Neslen Formation, Utah, USA. Journal of Sedimentary Research, 87 (2). pp. 168-187. ISSN 1527-1404

https://doi.org/10.2110/jsr.2017.7

Response of a Coal-Bearing Coastal Plain Succession to Marine Transgression: Campanian Neslen Formation, Utah, USA

Running Title: Marine transgression in coal-bearing coastal plain successions

Michelle N. Shiers*, David M. Hodgson, Nigel P. Mountney

*Fluvial Research Group, School of Earth and Environment, University of Leeds, Leeds, LS2 9JT, UK

* Corresponding author

ABSTRACT

The process regime of low-gradient coastal plains, delta plains and shorelines can change during transgression. In ancient successions, accurate assessment of the nature of marine influence is needed to produce detailed paleogeographic reconstructions, and to better predict lithological heterogeneity in hydrocarbon reservoirs. The Campanian lower Neslen Formation represents a fluvial-dominated and tide- and wave-influenced coastal-plain and delta-plain succession that accumulated along the margins of the Western Interior Seaway, USA. The succession records the interactions of multiple coeval sedimentary environments that accumulated during a period of relative sea-level rise.

A high-resolution data set based on closely spaced study sites employs vertical sedimentary graphical logs and stratigraphic panels for the recognition and correlation of a series of stratal packages. Each package represents the deposits of different paleoenvironments and process regimes within the context of an established regional sequence stratigraphic framework. Down-dip variations in the occurrence of architectural elements within each package demonstrate increasing marine influence as part of the fluvial-to-marine- transition zone.

Three marine-influenced packages are recognized. These exhibit evidence for an increase in the intensity of marine processes upwards as part of an overall transgression through the lower Neslen Formation. These marine-influenced packages likely correlate down-dip to flooding surfaces within the time-equivalent Îles Formation. The stratigraphic arrangement of these packages is attributed to minor rises in sea level, the effects of which were initially buffered by the presence of raised peat mires. Post-depositional auto-compaction of these mires resulted in marine incursion over broad areas of the coastal plain. Results demonstrate that autogenic processes modified the process response to overall rise in relative sea level through time. Understanding the complicated interplay of processes in low-gradient, coal-bearing, paralic settings requires analysis of high-resolution stratigraphic data to discern the relative role of autogenic and allogenic controls.

KEY WORDS:

Mesaverde, sequence stratigraphy, autogenic, allogenic, fluvial-to-marine transition

INTRODUCTION

Stratigraphic successions of mixed fluvial and marginal marine (paralic) origin, in which sediments are delivered by rivers and redistributed by waves and tides, accumulate during periods of high sea level stand and represent important archives of shoreline responses to sea-level change (Coleman and Wright 1975; Galloway 1975; Boyd et al. 1992; Ainsworth et al. 2011). Many modern coastal systems are undergoing transgression, and sedimentary process regimes vary systematically through the fluvial-to-marine transition zone (FMTZ) (Fedo and Cooper 1990; Boyd et al. 1992; Dalrymple and Choi 2007; Martinus and Gowland 2011) (Fig. 1). Studies of ancient transgressive paralic successions (e.g. Devine 1991; Valasek 1995; Sixsmith et al. 2008; Kieft et al. 2011; Leva Lopez et al. 2016) help to constrain the long-term sedimentary and stratigraphic response of FMTZs to autogenic and allogenic controls.

In ancient transgressive paralic successions, numerous allogenic and autogenic factors influence the interplay of fluvial, tidal and wave processes. Allogenic factors include tectonic setting, shelf width, climate, sediment supply rate and delivery mechanism, sea-level rise, and ocean basin morphology (Coleman and Wright 1975; Galloway 1975; Boyd et al. 1992; Bhattacharya and Giosan 2003; Nyberg and Howell 2016). Autogenic processes include switching of delta lobes (Coleman 1988; Tornqvist et al. 2008; Blum and Roberts 2012), autostratigraphy (Muto 2001; Muto and Steel 2002; Muto et al. 2007) and channel avulsion (Allen 1965; Richards et al. 1993; Stouthamer et al. 2011). However, unravelling the relative influence of autogenic and allogenic processes is a challenge and the interpretation of paralic strata which takes into account the influence of autogenic processes is lacking.

In paralic successions, the tracing of flooding surfaces up-dip into the non-marine realm requires careful consideration. Correlative surfaces to marine flooding surfaces in the coastal plain realm can be expressed by deposits that record marine influence (McLaurin and Steel 2000), or are absent through up-dip erosion by fluvial processes (Yoshida et al. 1996; Hettinger and Kirschbaum 2003). A notable autogenic control in many low-latitude paralic systems is the development of peat mires (Frazier and Osanik 1969; Fielding 1987; Bohacs and Suter 1997; Davies et al. 2006; Jerrett et al. 2011a, b). Prior to compaction, topographically elevated peat mires can act as buffers to limit transgression; raised mires develop above the level of fluvial or marine inundation (Eble et al. 1994; Kamola and Van Wagoner 1995; Jerrett et al. 2011a) and the cohesive nature of the sediment that comprises such bodies means that they are able to withstand erosional processes (McCabe 1985). Volume reduction associated with the auto-compaction of mires upon initial burial, and their transformation to coal, typically occurs rapidly (Ryer and Langer 1980; Fielding 1985; Courel 1987; Bohacs and Suter 1997; Nadon 1998; Holz et al. 2002). Hence, such processes cause significant local variations in accommodation. Localized areas of enhanced accommodation may be filled by fluvial crevasse-splay deposits (van Asselen et al. 2009), or may result in marine incursion anomalously far inland (Kosters and Bailey 1983; Kamola and Van Wagoner 1995; Jerrett et al. 2011a, b). Understanding the origin of flooding surfaces is important in extending sequence stratigraphic interpretations up-dip from the coastal realm. Such interpretations are especially important to improve prediction of the distribution of reservoir-quality sandbodies in transgressive settings.

The Campanian lower Neslen Formation (upper Mesaverde Group), Book Cliffs, eastern Utah, the focus of this work, records accumulation in the lower part of a coastal plain and delta-plain system (Young 1955; 1957; Fisher et al. 1960; Keighin and Fouch 1981; Franczyk et al. 1990; Willis 2000; Hettinger and Kirschbaum 2003; Kirschbaum and Hettinger 2004; Cole 2008; Shiers et al. 2014; Olariu et al. 2015; Colombera et al. 2016). The well-established regional sequence stratigraphic framework (Fig. 2), extensive marker beds that subdivide the stratigraphy (Fig. 3), and outcrops with strike- and dip-oriented control permit a rare opportunity to document the preserved record of mixed process response of coal-bearing paralic successions during an episode of overall transgression. Specific objectives are as follows: (i) to explain the origin of the preserved depositional architecture that arose in response to multiple laterally extensive, small scale relative sea-level rises; and (ii) to discuss the interplay of autogenic and allogenic controls on the sedimentary evolution of low-gradient coal-bearing paralic successions during transgression.

GEOLOGICAL SETTING

The Upper Mesaverde Group is exposed along the Book Cliffs of eastern Utah and western Colorado. It comprises stratal successions of shallow-marine, coastal and fluvial origin that accumulated during the Late Campanian (~72 Ma) as part of a clastic wedge that prograded eastwards from the Sevier Orogenic Belt towards the Western Interior Seaway (WIS) (Kauffman 1977; Miall et al. 2008). The western coastline of the WIS was oriented north-south, although many local embayments are postulated (Robinson Roberts and Kirschbaum 1995; Miall et al. 2008). The coastal plain was low gradient (2.5×10^{-4} m/m; Colombera et al. 2016) and low relief (Cole and Cummella 2003), meaning that minor relative sea-level rise resulted in widespread transgression or re-exposure of the coastal plain during regression. The seaway is estimated to have had a microtidal range of 0 to 2 m (Steel et al. 2012).

A sequence stratigraphic framework for the Mesaverde Group is well established (Figs. 2, 3) (e.g. Miall 1993; O'Byrne and Flint 1995; Olsen et al. 1995; Willis 2000; Yoshida 2000; Miall and Arush 2001; Davies et al. 2006; Rittersbacher et al. 2014). The Buck Tongue, stratigraphically above the Castlegate Sandstone (Figs. 2, 3A), records an abrupt landward shift in deposition due to either tectonic subsidence or an increase in relative sea level (Willis and Gabel 2003). Above this, renewed progradation of the clastic wedge (Wedge B; Aschoff and Steel 2011a) resulted in accumulation of the upper Mesaverde Group: the Sego Sandstone, Neslen Formation, Bluecastle Tongue, Tusher Formation, and Farrer Formation

(McLaurin and Steel 2000; Willis and Gabel 2001, 2003). The regional sequence stratigraphic framework of the Upper Mesaverde Group from Tusher Canyon (Utah) down-dip (i.e. eastwards) to Book Cliffs Mine, Grand Junction (Colorado) has been established by previous workers (e.g. McLaurin and Steel 2000; Hettinger and Kirschbaum 2002; Kirschbaum and Hettinger 2004; Kirschbaum and Spear 2012; Shiers et al. 2014) (Fig. 2).

Sequence stratigraphic interpretations of the Neslen Formation vary; figure 2 presents a generalized panel that is a compilation of these interpretations. The position of sequence boundaries within the Neslen Formation is contentious: Yoshida et al. (1996) argued for a sequence boundary in the lower part of the formation; McLaurin and Steel (2000) and Hettinger and Kirschbaum (2003) argued for a sequence boundary in the middle to upper part. Willis 2000 interprets the entire lower Neslen Formation as a lowstand systems tract (LST), with no sequence boundaries identified. Kirschbaum and Hettinger (2004) identify a thin shoreface sandstone in Colorado, the base of which they interpret as a Maximum Flooding Surface (MFS); coastal plain strata below this shoreface sandstone are assigned to a transgressive systems tract (TST). This shoreface sandstone is likely equivalent to the laterally extensive Thompson Canyon Sandstone Bed (TCSB) present in the vicinity of this study, which is also of marine shoreface origin (Kirschbaum and Spear 2012; Cole 2008; Shiers et al. 2014). The TCSB is recognized in Utah sections of the Neslen Formation between Horse Canyon and Buck Canyon, a distance of 45 km (Gualtieri 1991), and the base is interpreted as a MFS (Cole 2008). Strata of the lower Neslen Formation below the MFS represented by the TCSB are therefore assigned to a TST, whereas overlying strata of the upper Neslen Formation are assigned to a highstand systems tract (HST) (Fig. 2).

The Neslen Formation has been subdivided into three zones based on the occurrence of coal and laterally extensive tabular sandstone bodies (Shiers et al. 2014; Figs. 2, 3B). The lower two – the Palisade and Ballard zones – are the focus here. The lowermost Palisade Zone (Fig. 3B) is dominated by coal, siltstone and mudstone of fluvial floodplain origin, with rare channelized sandstone, coarsening-upwards sandstones and inclined heterolithic strata (Shiers et al. 2014). The overlying Ballard Zone is composed almost exclusively of coal and organic-rich mudstone and siltstone, and is bounded by two prominent tabular sandstone elements (Table 1): the lower Basal Ballard Sandstone Bed (BBSB) and the upper TCSB. The TCSB has been variably interpreted as representing a beach or tidal flat (Kirschbaum and Hettinger 2004), tidal bars (Hettinger and Kirschbaum 2002); a marine sandstone bounded at its base by a transgressive surface of marine erosion (Cole 2008). The TCSB was identified in all sections of this study, implying lateral continuity over this distance (Figs. 2, 3B). The BBSB was first identified by Shiers et al. (2014) and can be identified in all but one section in this study. The Chesterfield Zone – the uppermost of the three zones – overlies the TCSB and represents the upper part of the Neslen Formation. The Chesterfield Zone is composed dominantly of fluvial channel sandstones that become increasingly amalgamated upwards (Shiers et al. 2014). The Neslen Formation is overlain unconformably by the Bluecastle Tongue or conformably by the Farrer Formation (Figs. 2, 3) (Cole 2008; Lawton and Bradford 2011).

The lower Neslen Formation (below the base of the TCSB; Fig. 2) (Pitman et al. 1986; Franzcyk et al. 1990; Gualtieri 1991; Robinson Roberts and Kirschbaum 1995; Willis 2000; Hettinger and Kirschbaum 2002; Kirschbaum and Hettinger 2004; Cole 2008; Shiers et al. 2014; Olariu et al. 2015; Colombera et al. 2016), represents a tide- and wave-influenced coastal plain and delta-plain succession, which accumulated landward of a wave-dominated shoreline located in what is now western Colorado: the Îles Formation (Figs. 2, 3) (Kirschbaum and Hettinger 1998; Willis and Gabel 2003). The strata of the lower Neslen Formation pass basinward into time equivalent strata of the Îles Formation (Corcoran and Cozzette members) (Kirschbaum and Hettinger 2004) (Fig. 2).

METHODS

Thirteen study areas have been analyzed over a 21 km-long dip section (Floy Canyon to Sagers Canyon; Fig. 4). Sedimentary logs collected through the lower Neslen Formation (i.e. the Palisade and Ballard zones; Fig. 3) have been projected onto an east-to-west transect aligned oblique or perpendicular to the shoreline of the Western Interior Seaway (Robinson Roberts and Kirschbaum 1995; Aschoff and Steel 2011b) (Figs. 4, 5). In total, forty-two vertical sedimentary profiles (total length = 840 m), 106 stratigraphic panels that record stratigraphic architectural relationships (total width = 5000 m) and 408 paleocurrent readings (measured from cross-bedded sets, ripple laminations, scour marks and lateral accretion surfaces) were collected from the base of the Neslen Formation to the top of the TCSB.

Each log records lithofacies and ichnological information (Figs. 5, 6). In total, nine architectural elements (Fig. 7) have been interpreted in the lower Neslen Formation (cf. Shiers et al. 2014) from the vertical and lateral distribution of facies and their stratigraphic context as recorded on the stratigraphic panels; these are described in Table 1. Architectural elements comprise bodies of strata interpreted to represent the following sub-environment types: distributary channels (S_1); fluvial point bars that are sandstone dominated (S_2); fluvial (tidally influenced) point bars which are heterolithic (S_3); bay-head deltas (S_4); tabular reworked barrier sandstones (S_5); bay-fill sandstones (including mouth bars) (S_6); fluvial overbank (F_1); fine grained, fining upwards siltstone and mudstone of lagoonal or fluvial floodplain origin (F_2); and coal-prone mires (F_3) (Fig. 7).

Through identification of key stratal surfaces and coal zones within the stratigraphy, it is possible to correlate seven lithostratigraphic packages (Fig. 8), each of which represents time-equivalent depositional sub-environments. Correlation was refined through careful analysis of the facies within each architectural element, as well as their relationship to surrounding elements (Fig. 5). The depiction of the seven lithostratigraphic packages on a correlation panel

(Fig. 8) has been used to analyze the vertical and lateral changes in the proportions of constituent architectural elements (Fig. 9A). The proportion of architectural elements within each lithostratigraphic package is calculated from the cumulative logged thickness of each architectural element within that interval compared to the total sum of the thickness of the interval at each study site. Trends can also be established through analysis of, paleocurrent patterns within each interval (Fig. 9B), and the occurrence of sedimentary tidal and ichnological brackish water indicators (Fig. 9C). Paleogeographic maps (Fig. 9D) have been developed for each depositional interval. These have been constructed through analysis of the facies and architectural-element facies associations. Plan-view dimensions of elements were garnered from the lateral extent of elements on stratigraphic panels, and informed by imagery of modern systems.

RESULTS

Lower Palisade Zone

Description – The Lower Palisade Zone (average thickness 4.7 m) is the package from the top of the Sego Sandstone to the first coal bed in the Lower Neslen Formation (Fig. 8). The lower Palisade Zone is dominated by fine grained floodplain elements (F_2; 81 %), (Table 1; Fig. 9-1A), which contain abundant amber and compacted fragments of vegetation (which now appear as flattened clasts of coal), with rare overbank sandstones (F_1; Table 1; 7.5%). Laterally, the type of sandstone dominated elements within the Lower Palisade Zone varies (Fig. 8). At West Floy, small (up to 4 m thick and 150 m wide) heterolithic lateral accretion elements (Fig. 7B) are present (S_2; Table 1). Towards the east (East Salt Wash and Sagers Canyon), thin tabular sandstone elements (Fig. 7E) occur and are characterized internally by clinoforms that dip shallowly (<5°) towards the west (S_5; Table 1), and thicken- and coarsen-upwards. Sedimentary structures (Fig. 9-1C) observed in heterolithic lateral accretion elements (S_3) and tabular sandstone elements (S_5) (Table 1) notably include wavy and lenticular bedding (Fig. 6

A), and single and double mud draped ripples (Fig. 6 A, B). Paleoflow is predominantly towards the east (Fig. 9-1B).

Interpretation – In the western part of the study area, the fine grained elements are interpreted as part of a non-marine environment due to the presence of coal and amber (Fig. 7H) (cf. Guion et al. 1995). In the eastern part of the study area, however, the lack of these identifying features and indistinct bioturbation in some outcrops may indicate a lagoonal environment (Horne et al. 1978) (Fig. 5; Table 1). The inferred lateral change in environment from east to west is reinforced by the decrease in abundance of lateral accretion elements (S_2 and S_3) and the increase in occurrence of wave-dominated sandstones. Reworked barrier sandstone bodies (S_5) are interpreted as small back-stepping barrier complexes based on the architecture and the facies assemblages (Table 1), which were likely preserved via in place drowning as isolated ribbons (Fig. 8) (Sanders and Kumar 1975; Penland et al. 1988). Sandbodies in the lower Palisade Zone contain evidence of alternating current energy in the form of wavy and lenticular bedding, and single and double mud-draped ripples (Fig. 9-1C; Table 1). These sedimentary structures within sandstone-dominated elements, specifically the occurrence of double mud drapes, indicate current energies that fluctuated, possibly due to tidal forcing (Shanley et al. 1992; Lavigne 1999). The lower Palisade Zone is composed of deposits dominated by a fluvial process regime, although some marine-dominated elements do occur (e.g. S_5) they are present only in minor proportions (2%) and are restricted to the most easterly outcrops.

Palisade Coal Zone

Description – The Palisade Coal Zone lies stratigraphically above the Lower Palisade Zone (Fig. 8). It is characterized by coal-prone floodplain elements that comprise 26.5% of the package (Fig. 9-2A). Individual coal beds (Fig. 7I) vary in thickness, up to 1 m and are discontinuous at outcrop but can be traced laterally for 100s of meters at each study site. Fine grained elements

(F_2; Fig. 7G) are abundant in this package (46.5 %; Fig. 9-2A). Sandstone-prone elements such as bay-fill sandstones (S_6; 4%; Fig. 7F) and sandstone dominated lateral accretion (elements (S_2; 5.5%) are present in minor amounts (Fig. 9-2A). The type of sandstone-prone elements changes in a down-dip direction (i.e. to the east; Fig. 8) from lateral accretion elements (S_2) (Fig. 7B, C) (3 to 7 m thick), to large bay-fill sandstones up to 8m thick (S_6; Fig. 7F) and reworked barrier sandstones (S5; Fig. 7E). In the eastern part of the study area (Fig. 8; between East Sego to Sagers Canyon), mono-ichnospecific assemblages of ichnogenera such as *Rhizocorallium* are observed within bay-fill elements (S_6) and towards the top of heterolithic lateral accretion elements (S_3). Additionally, in this vicinity, *Teredolites* bored wood (Fig. 6E) is abundant at the base of these elements (S_3 and S_6) These elements are characterized by lithofacies defined by the following types of sedimentary structures: uni- and bi-directional ripples draped with a combination of silt and carbonaceous material; lenticular, flaser, and wavy bedding (Fig. 5D); sets of uni-directional ripple strata that record sediment transport in opposing directions (Fig. 9-2C). Paleoflow directions are dominantly towards the east and northeast (Fig. 9-2B).

Interpretation – The abundance of coal indicates the dominance of mires (cf. Davies et al. 2006), likely in a flood basin that additionally comprised fine grained siltstone and mudstone with minor sandstones of crevasse-splay origin (Table 1; Fig. 9-2D). Mires within the Neslen Formation are interpreted as partly ombrotrophic in origin (coals with mineral contents below 10 %, building up above flooding levels; Spears 1987; Davies et al. 2005). This interpretation of ombrotrophic mires is equivocal without detailed analysis of the inorganic mineral volume. However, this interpretation is supported by an important consideration: raised mires self-exclude clastic detritus and allow the organic material to develop good quality coals (such as those in the Neslen Formation, with low clastic content; Tabet et al. 2008) in close proximity to active clastic fluvial systems (Clymo 1987) (Table 1; Fig. 8). The same reasoning was used to support the interpretation of accumulation of coals in largely ombrotrophic mires within the underlying Blackhawk Formation (Davies et al, 2006). The Blackhawk Formation formed in similar depositional settings under similar climatic regimes to those of the Neslen Formation (Davies et al. 2006). The interpretation of ombrotrophic mires is important as they serve to stabilize fluvial channel position and limit channel migration (the majority of paleoflow orientations are directed towards the north and east (Fig. 9-2B). The observed trace fossils, their lack of diversity and diminutive size of their occurrence within architectural elements towards the east of the studied section (Figs. 5, 8) is indicative of an environment that was subject to brackish-water influence (Bromley 1996; Gingras et al. 2012). Drapes on ripple foresets and opposing directions of currents recorded by current ripple cross-laminated strata can be interpreted as having been modified by tides (Shanley et al. 1992). Symmetrical ripples are interpreted as wave ripples generated on the bottom of a standing body of water (De Raaf et al. 1977). In this case, the association of symmetrical ripples with brackish-water ichnogenera indicates an environment of deposition such as a lagoon.

Middle Palisade Zone

Description – This package (Fig. 8) is dominated by a range of sandstone-prone elements (66 %; Fig. 9-3A), subordinate fine-grained elements commonly contain plant debris (as fragments of flattened coal) and rooted horizons in the west. Sandstone-prone (S_2; Fig. 7B) and heterolithic (S_3; Fig. 7C) lateral accretion elements occur predominantly in the west, whereas bay-fill sandstone elements up to 10 m thick (S_6; Fig. 7F) and tabular barrier sandstone elements up to 6 m thick (S_5; Fig. 7E) are more common in the east (Fig. 8). Tabular sandstone elements can be traced laterally for up to 500 m in dip-oriented sections (average 300 m). A variety of trace fossils characterize the Middle Palisade Zone, notably *Arenicolites*, *Teredolites* (Fig. 6E), *Ophiomorpha* (Fig. 6F), *Rhizocorallium,* with an increase in bioturbation intensity and diversity towards the east, from 1 to 5 (Taylor and Goldring 1993). Trace fossils commonly occur as mono-ichnospecific assemblages towards the top of beds and are of a limited size but a high density. Within all sandstone elements (S_2 to S_6), silt-draped ripples are abundant (Fig. 6A, B), as are lenticular, wavy and flaser bedding (Figs. 6A, 9-3C), and rare symmetrical ripple lamination (Fig. 9-3C). Where more than one sandstone-dominated element is observed within the Middle Palisade Zone, the lowermost element is either a bay-fill or barrier sandstone element (S_5 or S_6), and the upper is either a sandstone-prone or heterolithic lateral accretion element (S_2 or S_3) (e.g. West Crescent Mine and East Salt Wash). Paleocurrents in this package (Fig. 9-3B) show a wide range: the dominant direction is towards the SE, with subordinate trends to the north and south.

Interpretation – The dominant depositional environment interpreted from both the ichnological assemblage, density and size of traces is a brackish-water to marine setting (Bromley 1996; Gingras et al. 2012), although *Teredolites* can be rafted up-stream into fresh water settings (Shanley et al. 1992; Lavigne 1999). Sedimentary structures indicative of tidal influence (Shanley et al. 1992) occur within sandstones throughout this package and are present at the most up-dip localities (West Floy; Fig. 5). Fine grained elements (F_2; Table 1) in this package are indicative of either floodplain or lagoonal environments, depending on the presence or absence of plant material with rooted horizons, or bioturbation indicative of the terrestrial nature of siltstone and mudstone beds (Horne et al. 1978; Guion et al. 1995) (Table 1). The reworked barrier elements (S_5) are interpreted as minor washover fans constructed from a distal barrier or spit and preserved via in-place drowning (Sanders and Kumar 1975; Penland et al. 1988) (Table 1; Fig. 9-3D). The wide variability of paleocurrents (Fig. 9-3B) is attributed to a combination of flow reversals within channelized elements (S_2, S_3) and the sinuous nature of the channels and modification at the shoreline, for example by longshore currents (Fig. 9-3D) (Shanley et al. 1992; Bhattacharya and Giosan 2003). The change in process influence between lower and upper elements within the Middle Palisade Zone, with underlying elements being more marine influenced and upper elements more fluvial influenced, is interpreted to record an initial marine incursion and the subsequent filling of accommodation in response to progradation of fluvial systems as part of a transgressive interval (Fig. 9).

The wide range of architectural elements (S_2 to S_6) within the Middle Palisade Zone is indicative of modification by a variety of combinations of fluvial, wave and tide processes (Table 1). There is a down-dip change in architectural elements whereby, towards the west, fluvial elements (S_{2-3}) occur encased within floodplain fines (F_2; Table 1), whereas to the east marine influenced elements are encased within fine grained lagoonal deposits (Figs. 5, 8). The spatial variability of multiple coeval sub-environments likely records the interplay of fluvial, wave and tidal processes.

Upper Palisade Zone

Description – This package (Fig. 8) is dominated by fine-grained deposits (66%; F_2), overbank sandstones (5%; F_1; Fig. 7G), lateral accretion elements (24%; S_2 and S_3; Figs. 7B, C; 9-4A), and bay-fill sandstones (1%; S_6; Fig. 7E). Within this package, coal (4% overall) decreases in abundance to the east (Figs. 5, 8). The occurrence of sandstone dominated elements (S_2 and S_3) decreases to the east (Fig. 8). Paleocurrents exhibit wide variability (Fig. 9-4B) but are overall directed towards the east. Sedimentary structures include lenticular bedding, mud and carbonaceous draped ripple forms (Fig. 6A) and *Teredolites* bored wood (Fig. 6E) within the basal-most parts of lateral accretion elements (S_2; Fig. 9-4C).

Interpretation – The paleoenvironment was dominated by a floodplain containing small raised mires traversed by small sinuous channels (Fig. 9-4D). Draped ripples present within sandstone-prone lateral accretion elements (S_2; Fig. 8) suggests fluctuating flow energies, which were likely caused by tidal or discharge variations (cf. Thomas et al. 1987). The decrease in the occurrence of lateral accretion deposits towards the east may be due to the line of outcrop failing to intersect major channel bodies (Fig. 9-4D). Alternatively, this may reflect lateral changes through the FMTZ. The presence of *Teredolites* indicates close proximity to a brackish environment, likely within the zone of tidal push (Shanley et al. 1992; Lavigne 1999).

Ballard Zone

Description – Occurring stratigraphically between the BBSB and TCSB (Fig. 8), this package has large proportions of coal (15%; F_3; Fig. 9-6A), with seams up to 3 m thick, which previous authors have named the Ballard Coal Zone (Cole 2008; Shiers et al. 2014). Within this package, there occur a high proportion of organic-prone, fine grained elements (67%; $F_{2;}$ Fig. 7H) cut by distributary channel elements (S_1), which are 3-7 m thick ($S_{1;}$ Table 1) and small (5 m thick) sandstone-prone lateral accretion elements (S_2), which together make up 15% of the package (Fig. 8). Within the distributary channel-fills (S_1) (Fig. 7A), carbonaceous and mud drapes on foresets and bottomsets of cross-beds, and rare mud drapes on ripple forms on the uppermost surface of the elements are observed (Fig. 9-6C). Paleocurrents within these bodies are aligned to the south and east (Fig. 9-6B), indicating that channel-fills are oriented in this direction, and are surrounded by dominantly coal-prone floodplain (F_2, F_3; Fig. 9-6D). Bioturbation (*Skolithos* and *Arenicolites, Thalassinoides*) are observed in abundance within mono-specific assemblages in the basal-most parts of elements, as are lags containing fossil wood debris with *Teredolites* (Fig. 6E).

Interpretation – Fine-grained deposits (F_2) in this package are interpreted to be of terrestrial origin due to the high organic content, as well as the presence of rooted horizons (Fig. 8). Distributary channel-fill elements are interpreted based on the arrangement of internal lithofacies and the external geometry of the sand bodies (Colombera et al. 2016) (Table 1). Ichnogenera present within the base of these channelized elements indicate deposition within marine-to-brackish water (Tonkin 2012). However, the majority of the channel-fills show little evidence of modification by marine processes. This may be due to overprinting of marine influence during river floods (Colombera et al. 2016). Sandstone-dominated lateral accretion elements (S_2) do not record indicators of marine influence, and are interpreted as meandering fluvial channels, possibly tie channels between larger distributary channels (Fig. 9-6D) within a delta-plain setting. Overall this package is interpreted as fluvially dominated with some minor modification by tides within the lower parts of distributary channel fills.

Basal Ballard and Thompson Canyon Sandstone Beds

Description – Bounding the Ballard Zone at the base is the Basal Ballard Sandstone Bed (BBSB) and at the top is the Thompson Canyon Sandstone Bed (TCSB); both form distinctive tabular marker sandstone bodies (Table 1; Fig. 6E). The TCSB is made up of a lower fine-grained package and an upper tabular sandstone body (Table 1; Fig. 5). Together, they are commonly bounded above and below by coals (Figs. 5, 8, 10B). Paleocurrents measured from ripple forms in the BBSB and TCSB are predominantly directed towards the southeast and east, respectively (Fig. 9-5B, 7B). The BBSB pinches out between the East Floy and West Floy study sites over a distance of 2.5 km (Fig. 8). This pinch-out is marked at West Floy by a thin siltstone between two coal beds; the siltstone contains a mono-species assemblage of *Arenicolites* of diminutive size.

The lower portion of the TCSB has abundant *Thalassinoides* (Fig. 6D) directly below the base (Fig. 5). The lower part of the TCSB is fine-grained and heavily bioturbated, masking any original sedimentary structures (Table 1). Bioturbation within the reworked barrier sandstone elements (S_5), including the upper portion of the TCSB, comprises *Ophiomorpha* (Fig. 6F), *Planolites*, *Bergaueria,* and *Arenicolites*, which increase in intensity and abundance towards the east. Sedimentary structures within sandy portions of the BBSB and TCSB include low angle laminations, symmetrical ripple lamination, and asymmetrical ripple lamination that exhibits both single and double mud and silt drapes in the lowermost beds of the element (S_5; Table 1).

Interpretation – The ichnology of the siltstone that marks the pinch-out of the BBSB around Floy Canyon is low diversity and traces are of a limited size, therefore most likely representing a marine or brackish environment (cf. Tonkin 2012). The increase in intensity and diversity of the bioturbation within the BBSB and TCSB (increasing towards the east from a BI of 1 to 5; Fig. 6F) indicates an environment that became increasingly marine influenced with more stable salinity to the east (cf. Bromley 1996; Tonkin 2012). The sedimentary structures in the TCSB and BBSB (Table 1) indicate the influence of wave processes, with drapes on the ripples indicative of tidal influence.

The lower portion of the TCSB is interpreted as lagoonal or interdistributary bay fines, whilst the upper part and the BBSB are interpreted as part of a back-stepping barrier complex (Table 1). Preservation of the unit indicates that transgressive submergence (cf. Penland et al. 1988), in-place drowning (cf. Sanders and Kumar 1975) or shoreface retreat (cf. Penland et al. 1988) of the barrier complex has occurred. The style and stratigraphic expression of barrier retreat, or rollover, is controlled by the interplay of substrate slope, sediment supply, rate of sea-level rise and back-barrier accommodation (Mellett et al. 2012). Where barriers are drowned in place then sands would be preserved as isolated ribbons at successive locations (Sanders and Kumar 1975), counter to the laterally extensive sandbodies of the BBSB and TCSB. Barrier rollover retreat leads to the formation of a sand blanket that infills the back barrier and overlying lagoonal sediments. Barrier retreat is most commonly associated with an erosional unconformity or ravinement surface (Cattaneo and Steel 2003), such surfaces are not observed within the Lower Neslen Formation. Transgressive submergence is therefore the most likely mode of preservation of shelf sand bodies (barrier complexes and sheet sands) without the preservation of the shoreline sands these bodies were derived from (Penland et al. 1988). Such sand bodies preserved via transgressive submergence likely accumulated down-drift of transgressed delta complexes.

DISCUSSION

Stratigraphic variations

Vertical and lateral trends within and between the depositional packages are important in understanding the temporal and spatial variations in the sedimentary succession. Within the majority of depositional packages, there is a down-dip variability in architectural elements from dominantly fluvial with higher proportions of coal dominated elements, to architectural elements which exhibit marine influence encased within coal-poor, fine-grained mudstone and siltstone (Figs. 5, 8). The Middle Palisade Zone (MPZ) records a change from dominantly fluvial elements encased within floodplain fines in the west, to marine-influenced elements encapsulated by fine-grained elements of lagoon origin in the east (Fig. 9-3D). Packages were increasingly influenced by marine processes towards the east as part of the FMTZ (Fig. 1C). The preserved stratigraphic signature of the FMTZ is not simple. Architectural elements deposited within a depositional package were not necessarily coeval. Examination of the relative change in elements, sedimentary structures and ichnology (Fig. 5) recorded at study locations in close proximity to each other are required to recognize these changes. Stratigraphically, the paleoenvironment changes from a fluvial dominated delta plain, which is influenced to some extent by tidal processes, to a wave dominated shoreline system (Fig. 9D).

The sandstone dominated MPZ contains abundant marine indicators (Figs. 5, 9-3C) within a thin interval (8 m average thickness) and lies stratigraphically between the Palisade Coal Zone and Upper Palisade Zone, which themselves contain relatively fewer marine indicators within sandstone elements (Fig. 9C). Architectural elements within the MPZ record significant spatial variability (Fig. 9-3D) within an overall shallowing upwards trend, which continues into the Upper Palisade Zone (Fig. 8). The MPZ records deposition within a lower delta-plain setting that was substantially modified by marine processes, given the presence of structures indicative of tidal influence as well as brackish water ichnology. This markedly marine-influenced package occurs at a point in the stratigraphy that is not accounted for by previous sequence stratigraphic interpretations (Fig. 2). The BBSB and TCSB are interpreted as variably wave-dominated, back-stepping barrier complexes (Sanders and Kumar 1975; Penland et al. 1988). The greater thickness and extent of the TCSB, together with the more intense bioturbation, and the occurrence of trace fossils such as *Ophiomorph*a (Fig. 6F), are indicative of greater open-marine conditions than the BBSB. This shows that, overall, the MPZ, BBSB and TCSB become increasingly modified by marine processes upwards (Fig. 10).

Marine-influenced packages

Prediction of the way in which marine-influenced packages correlate with down-dip flooding surfaces and shoreface deposits, and prediction of shorefaces and controls on their occurrence within the stratigraphy, is important for gaining an improved understanding of the way in which coastal plains respond to sea-level change. The controls on the occurrence and position of the MPZ, BBSB and TCSB can be attributed to autogenic or allogenic processes, as considered below.

Allogenic processes – Correlations of the lower Neslen Formation indicate that the TCSB is contiguous to the tongue of mudstone between the Corcoran and Cozzette members of the Îles Formation (Kirschbaum and Spear 2012; MFS 3: Fig. 2). The base of the TCSB is interpreted as the MFS. This is supported by the sharp contact of the lower TCSB which has abundant *Thalassinoides* directly below its base (Fig. 6D), a thickening and coarsening upward trend within the TCSB, and an underlying, well-developed coal seam (Fig. 10B). The base of the TCSB represents an abrupt and significant deepening in depositional environment from peat mire to lagoonal fines and wave-modified sandstone (Fig. 10). The base of the BBSB, which has a lateral extent of at least 18 km, displays a facies dislocation at its base from coal to wave-modified sandstone (S_5). Additionally, it possesses a similar internal lithofacies composition and architecture to the TCSB, and therefore likely represents a minor flooding surface (FS; Fig. 10).

The MPZ contains a wide range of architectural elements, which contain abundant evidence for marine influence. As a marine-influenced package additional to, and lower in the stratigraphy than, the BBSB and TCSB, it is likely that this package correlates down dip to minor tongues of the Mancos Shale within the Corcoran Member (Fig. 2); this correlation has not been previously proposed. The marine incursion responsible for deposition of the MPZ is therefore interpreted as the most landward expression of transgression that was on-going further seaward (cf. Rudolph et al. 2015), similar to that described in the Castlegate Formation (McLaurin and Steel 2000).

The successive increase in marine processes preserved upwards from the MPZ to the BBSB and ultimately to the TCSB indicates that the lower Neslen Formation records an overall episode of transgression punctuated by variations in the rate of sea-level change or in sediment supply, which modify the rate of transgression (Fig. 10A). No relative sea-level fall is interpreted between flooding surfaces, rather a decrease in rate of relative sea-level rise relative to the rate of sediment supply results in the deposition of regressive, progradational intervals (Figs. 9, 10A). The low gradient of the coastal delta plain (Colombera et al. 2016) means that even minor relative sea-level rise would flood broad portions of the coastal plain. The refined stratigraphic framework (Fig. 10A) exhibits a series of retrogradationally stacked wave-dominated sandstones within a net transgressive tract (Fig. 10C).

Autogenic processes – Autogenic processes such as coal compaction and delta auto-retreat are important considerations when analyzing the cause of overall transgression within a paralic succession.

Marine-influenced packages (MPZ, BBSB and TCSB) may have been produced by purely autogenic processes intrinsic to the evolution of the system. These packages may be referred to as 'auto-breaks' within an overall progradational sequence (Fig. 2) which was subject to autoretreat (the landward retreat of a shoreline which occurs inevitably, under conditions of constant rate of relative sea-level rise and without change in basin conditions: Muto and Steel 1992; 1997).

The MPZ and TCSB are underlain by coal zones, and the BBSB is underlain by coal in four up-dip and central localities (Fig. 8). The distribution of coal through the Neslen Formation can be used to explain the location of marine-influenced packages, as well as their thickness and internal character. It is common for significant coal deposits to accumulate above and landward of shoreface sandstone bodies (Ryer 1981; Cross 1988; Jerrett et al. 2011a, b). This suggests that the up-dip limit of shorefaces (i.e. the extent of transgression) is defined by the seaward-most position of raised coal mires. This is because raised mires withstand erosion and hence are able to buffer transgression (McCabe 1985; Kamola and Van Wagoner 1995; Jerrett et al. 2011b). Mires and swamps in coastal-plain and delta-plain settings can rapidly compact to a level that is equal to or lower than sea level (e.g. Mississippi region – St Bernard and Lafourche deltas; Blum and Roberts 2009; California – Sacramento-San Joaquin Delta; Miller et al. 2008; Ganges–Brahmaputra Delta; Schmidt 2015). Auto-compaction of coal occurs rapidly following deposition (Fielding 1984; 1985; Nadon 1998; Ryer and Langer 1980; Courel 1987), which encourages marine inundation over broad areas of the coastal plain adjacent to sites of clastic accumulation that compact less (Kosters and Bailey 1983; van Asselen et al. 2009; Jerrett et al. 2011a, b). Such a process means that transgression in response to low-amplitude sea-level rise can occur passively (i.e. with low energy) over a low-relief and low-gradient coastal plain. This differential compaction can also explain the juxtaposition of architectural elements observed within the Neslen Formation (e.g. MPZ; Fig. 9-3D) and the occurrence of marine-influenced or marine-dominated intervals (MPZ, BBSB and TCSB; Figs. 8, 10). Differential compaction, and the subsequent filling of the newly generated accommodation might also play a role in sediment partitioning by reducing the delivery of sediment to the shoreline, and hence decreasing the rate of delta or shoreface progradation and favoring barrier preservation in a similar way to the behavior of local accommodation created by growth faults proximal to the shelf edge (cf. Olariu and Olariu 2015).

Relative sea-level rise may be driven by autogenic coal compaction, rather than eustatic sea-level change. This is notably evident in the MPZ, where more than one architectural element is observed, the lower is more influenced by marine processes (Figs. 8, 10). The thickness of coal seams is greatest where there is no underlying sandstone (e.g. Palisade Coal Zone at East Floy) and thinnest where sandstone-dominated elements occur (e.g. Ballard Coal Zone at Right Hand Crescent). This is due to differential rates and amounts of compaction of sandstone-prone elements compared to fine-grained and coal-prone elements (F_2 and F_3). A sandstone element (S_1 to S_6) will undergo less post-depositional compaction than an adjacent fine-grained elements (F_2 and F_3). As such, the accommodation generated after deposition will be greatest above a fine grained, or coal prone element. Where coal fills this accommodation, the deposits will be thinner where they overlie a sandstone-prone element (Fig. 8). Differential compaction explains why the MPZ, BBSB and TCSB are thickest where they overly thick coal accumulations in place where they show an increase in abundance of marine indicators (Figs. 8, 10B).

CONCLUSIONS

Use of a high-resolution dataset has allowed the correlation of paralic strata within the coal-bearing lower Neslen Formation. This method has enabled recognition of discrete stratal packages within an ancient low-gradient, low-relief coastal plain and shoreline succession, which records sedimentological and stratigraphical evidence for modification by interplay of fluvial, wave and tidal processes.

Correlation of marine-influenced packages helps to refine the established sequence stratigraphic framework, which overall indicates that the lower Neslen Formation accumulated as part of a long-term TST. The deposition and preservation of three marine influenced packages (MPZ, BBSB and TCSB) arose in response to three laterally extensive, but small scale cycles of sea-level change, which increased in amplitude over time (i.e. upwards in the succession). The base of the TCSB marks a regional maximum flooding surface, which likely correlates down-dip to a tongue of Mancos Shale between the Corcoran and Cozzette members of the Îles Formation of open marine origin. The BBSB and MPZ record minor floods across the coastal plain as part of an overall episode of punctuated relative sea-level rise.

The impact of peat-developing environments in low-gradient coastal plains is significant. Peat mires initially act as buffers to sea-level rise. Following deposition, auto-compaction of peat during its transformation to coal reaches a threshold level beyond which widespread marine incursion may occur rapidly over the coastal plain. Lateral variability in the distribution of peat mires across a low-gradient coastal plain result in shifting patterns of accommodation generation. This may result in the juxtaposition of a broad range of depositional environments, leading to the preservation of complicated facies patterns and architectural relationships.

Overall, this study shows that the interplay of autogenic and allogenic controls on the sedimentary evolution of the succession is complicated. The role of autogenic processes, such as coal compaction, is often overlooked but the rate and extent of marine transgression associated with moderate relative sea-level rise in low-gradient, low relief coastal settings may be driven by auto-compaction of peat mires in the coastal plain.

ACKNOWLEDGEMENTS

This research was funded by Areva, BHPBilliton, ConocoPhillips, Det norske oljeselskap ASA, Murphy Oil, Nexen, Saudi Aramco, Shell, Tullow Oil, Woodside and YPF through their sponsorship of the Fluvial & Eolian Research Group at the University of Leeds. Tom Wiggins, Sarah Cobain, Luke Beirne and Camille Dwyer are thanked for their help and assistance in the field. Rhodri Jerrett is thanked for helpful discussions. Reviews by Christopher Fielding, Cornel Olariu and an anonymous reviewer together with associate editor Tobi Payenberg have greatly improved the manuscript.

REFERENCES

AINSWORTH, R.B., 2010, Prediction of stratigraphic compartmentalization in marginal marine reservoirs: Geological Society, London, Special Publications, v. 347, p. 199-218.

AINSWORTH, R.B., FLINT, S.S., and HOWELL, J.A., 2008, Predicting coastal depositional style: influence of basin morphology and accommodation to sediment supply ratio within a sequence stratigraphic framework: Recent Advances in Models of Siliciclastic Shallow-Marine Stratigraphy: SEPM, Special Publication, v. 90, p. 237-263.

AINSWORTH, R.B., VAKARELOV, B.K., and NANSON, R.A., 2011, Dynamic spatial and temporal prediction of changes in depositional processes on clastic shorelines: Toward improved subsurface uncertainty reduction and management: AAPG Bulletin, v. 95, p. 267-297.

ALLEN, J.R., 1965, A review of the origin and characteristics of recent alluvial sediments: Sedimentology, v. 5, p. 89-191.

ASCHOFF, J., and STEEL, R., 2011a, Anomalous clastic wedge development during the Sevier-Laramide transition, North American Cordilleran foreland basin, USA: Geological Society of America Bulletin, v. 123, p. 1822-1835.

ASCHOFF, J., and STEEL, R., 2011b, Anatomy and development of a low-accommodation clastic wedge, upper Cretaceous, Cordilleran Foreland Basin, USA: Sedimentary Geology, v. 236, p. 1-24.

BHATTACHARYA, J.P., and GIOSAN, L., 2003, Wave-influenced deltas: Geomorphological implications for facies reconstruction: Sedimentology, v. 50, p. 187-210.

BLUM, M.D., and ROBERTS, H.H., 2009, Drowning of the Mississippi Delta due to insufficient sediment supply and global sea-level rise: Nature Geoscience, v. 2, p. 488-491.

BLUM, M.D., and ROBERTS, H.H., 2012, The Mississippi Delta Region: Past, Present, and Future: Annual Review of Earth and Planetary Sciences, v. 40, p. 655-683.

BOHACS, K., and SUTER, J., 1997, Sequence stratigraphic distribution of coaly rocks: fundamental controls and paralic examples: AAPG Bulletin, v. 81, p. 1612-1639.

BOYD, R., DALRYMPLE, R., and ZAITLIN, B.A., 1992, Classification of clastic coastal depositional environments: Sedimentary Geology, v. 80, p. 139-150.

BRIDGE, J., 2006, Fluvial facies models: recent developments, *in* Posamentier, H. W., Walker, R., G. eds. Facies models revisited: SEPM Special publications, v. 84, p. 85-117.

BROMLEY, R., 1996, Trace Fossils: Biology, Taphonomy and Applications Chapman Hall, London, 361 p.

CATTANEO, A., and STEEL, R.J., 2003, Transgressive deposits: a review of their variability: Earth-Science Reviews,v. 62,p. 187-228.

CLYMO, R., 1987, Rainwater-fed peat as a precursor of coal, *in* Scott, A.C., ed., Coal and Coal Bearing Strata: Recent Advances, Geological Society, London, Special Publications, p. 17-23.

COLE, R., 2008, Characterization of fluvial sand bodies in the Neslen and lower Farrer formations (Upper Cretaceous), Lower Sego Canyon, Utah, *in* Longman, M.W., and Morgan, C.D., eds., Hydrocarbons Systems and Production in the Uinta Basin, Utah, RMAG-UGA Publication 37, p. 81-100.

COLE, R., and CUMELLA, S., 2003, Stratigraphic architecture and reservoir characteristics of the Mesaverde Group, southern Piceance Basin, Colorado: Piceance Basin Guidebook, chapter. 18, p. 385-442.

COLEMAN, J.M., 1988, Dynamic changes and processes in the Mississippi River delta: Geological Society of America Bulletin, v. 100, p. 999-1015.

COLEMAN, J.M., and WRIGHT, L., 1975, Modern river deltas: variability of processes and sand bodies. Deltas: Models for Exploration, p. 99-149.

COLOMBERA, L., SHIERS, M.N., and MOUNTNEY, N., 2016, Assessment of backwater controls on the architecture of distributary channel fills in a tide-influenced coastal-plain succession: Campanian Neslen Formation, USA: Journal of Sedimentary Research, v. 86, p. 1-22.

COUREL, L., 1987, Stages in the compaction of peat; examples from the Stephanian and Permian of the Massif Central, France: Journal of the Geological Society, v. 144, p. 489-493.

CROSS, T., A., 1988, Controls on coal distribution in transgressive-regressive cycles, Upper Cretaceous, Western Interior, USA, *in* Wilgus, C. K., Hastings, B. S., Posamentier, H., Van Wagoner, J., Ross, C. A., Kendall, C. G., eds., Sea-level changes: an integrated approach: SEPM Special Publication, v. 42, p. 371-380.

DALRYMPLE, R.W., and CHOI, K., 2007, Morphologic and facies trends through the fluvial-marine transition in tide-dominated depositional systems: A schematic framework for environmental and sequence-stratigraphic interpretation: Earth-Science Reviews, v. 81, p. 135-174.

DAVIES, R., DIESSEL, C., HOWELL, J., FLINT, S., and BOYD, R., 2005, Vertical and lateral variation in the petrography of the Upper Cretaceous Sunnyside coal of eastern Utah, USA—implications for the recognition of high-resolution accommodation changes in paralic coal seams: International Journal of Coal Geology, v. 61, p. 13-33.

DAVIES, R., HOWELL, J., BOYD, R., FLINT, S., and DIESSEL, C., 2006, High-resolution sequence-stratigraphic correlation between shallow-marine and terrestrial strata: Examples from the Sunnyside Member of the Cretaceous Blackhawk Formation, Book Cliffs, eastern Utah: AAPG Bulletin, v. 90, p. 1121-1140.

DEVINE, P.E., 1991, Transgressive origin of channeled estuarine deposits in the Point Lookout Sandstone, northwestern New Mexico: A model for Upper Cretaceous, cyclic regressive parasequences of the U.S. Western Interior: AAPG Bulletin, v. 75, p. 1039-1063.

DE RAAF, J.F.M., BOERSMA, J.R., and VAN GELDER, A., 1977, Wave-generated structures and sequences from a shallow marine succession, Lower Carboniferous, County Cork, Ireland: Sedimentology, v. 24, p. 451-483.

EBLE, C. F., HOWER, J. C. and ANDREWS, W. M., 1994, Paleoecology of the Fire Clay coal bed in a portion of the Eastern Kentucky Coal Field: Palaeogeography, Palaeoclimatology, Palaeoecology, v. 106, p. 287-305.

Fedo, C.M., and Cooper, J.D., 1990, Braided fluvial to marine transition; the basal Lower Cambrian Wood Canyon Formation, southern Marble Mountains, Mojave Desert, California: Journal of Sedimentary Research, v. 60, p. 220-234.

Fielding, C.R., 1984, A coal depositional model for the Durham Coal Measures of NE England: Journal of the Geological Society, v. 141, p. 919-931.

Fielding, C.R., 1985, Coal depositional models and the distinction between alluvial and delta plain environments: Sedimentary Geology, v. 42, p. 41-48.

Fielding, C.R., 1987, Coal depositional models for deltaic and alluvial plain sequences: Geology, v. 15, p. 661-664.

Fisher, D.J., Erdmann, C.E., and Reeside, J.B.J., 1960, Cretaceous and Tertiary formations of the Book Cliffs, Carbon, Emery, and Grand Counties, Utah, and Garfield and Mesa Counties, Colorado.: Geological survey professional paper v. 332, 79p.

Franczyk, K., Pitman, J., and Nichols, D.J., 1990, Sedimentology, Mineralogy, Palynology, and Depositional History of some Uppermost Cretaceous and Lowermost Tertiary Rocks along the Utah Book and Roan Cliffs East of the Green River: U. S. Geological Survey Bulletin, v. 1787, p. 1-37.

Frazier, D.E., and Osanik, A., 1969, Recent Peat Deposits-Louisiana Coastal Plain: Geological Society of America Special Papers, v. 114, p. 63-86.

Galloway, W.E., 1975, Process framework for describing the morphologic and stratigraphic evolution of deltaic depositional systems, in Broussard, M.L., ed., Deltas – Models for exploration: Houston Geological Society, p. 87-98.

Gingras, M.K., MacEachern, J.A., Dashtgard, S.E., Zonneveld, J-P., Schoengut, J., Ranger, M.J., and Pemberton, S.G., 2012, Estuaries, *in* Knaust, D and Bromley, R.G., eds., Trace fossils as indicators of sedimentary environments: Developments in Sedimentology 64, Elsevier, p. 463-506.

Gualtieri, J.L., 1991, Map and cross sections of coal zones in the Upper Cretaceous Neslen Formation, North-Central part of the Westwater 30' * 60' quadrangle, Grand and Uintah counties, Utah: U.S. Geological Survey Coal Investigations Series, map C-133, 1 sheet.

Guion, P. D., Fulton, I. M., and Jones, N. S., 1995, Sedimentary facies of the coal-bearing Westphalian A and B north of the Wales-Brabant High: Geological Society, London, Special Publications,v. 82,p. 45-78.

Hettinger, R.D., and Kirschbaum, M.A., 2002, Stratigraphy of the Upper Cretaceous Mancos Shale (upper part) and Mesaverde Group in the southern part of the Uinta and Piceance basins, Utah and Colorado: Petroleum Systems and Geological Assessment of Oil and Gas in the Uinta-Piceance Province, Utah and Colorado: United States Geological Survey Digital Data Series DDS-69-B, chapter 12, p. 1-16.

Holz, M., Kalkreuth, W., and Banerjee, I., 2002, Sequence stratigraphy of paralic coal-bearing strata: an overview: International Journal of Coal Geology, v. 48, p. 147-179.

Horne, J., Ferm, J., Caruccio, F., and Baganz, B., 1978, Depositional models in coal exploration and mine planning in Appalachian region: AAPG Bulletin, v. 62, p. 2379-2411.

Jerrett, R.M., Flint, S.S., Davies, R.C. and Hodgson, D.M., 2011a, Sequence stratigraphic interpretation of a Pennsylvanian (Upper Carboniferous) coal from the central Appalachian Basin, USA: Sedimentology, v. 58, p. 1180-1207.

Jerrett, R.M., Hodgson, D.M., Flint, S.S., and Davies, R. 2011b. Control of Relative Sea Level and Climate on Coal Character in the Westphalian C (Atokan) Four Corners Formation, Central Appalachian Basin, USA: Journal of Sedimentary Research, v. 81, p. 420-445.

Joeckel, R., and Korus, J., 2012, Bayhead delta interpretation of an Upper Pennsylvanian sheetlike sandbody and the broader understanding of transgressive deposits in cyclothems: Sedimentary Geology, v. 275, p. 22-37.

Kamola, D.L., and Van Wagoner, J.C., 1995, Stratigraphy and facies architecture of parasequences with examples from the Spring Canyon Member, Blackhawk Formation, Utah, in Van Wagoner, J.C., and Bertram, G.T., eds., Sequence Stratigraphy of Foreland Basin Deposits AAPG, p. 27-54.

Kauffman, E.G., 1977, Geological and Biological Overview: Western Interior Cretaceous Basin: The Mountain Geologist, v. 14, p. 75-99.

Keighin, C.W., and Fouch, T.D., 1981, Depositional Environments and Diagenesis of some Nonmarine Upper Cretaceous Reservoir Rocks Uinta Basin Utah: SEPM Special Publication, v. 31, p. 109-125.

Kieft, R.L., Hampson, G.J., Jackson, C.A.-L., and Larsen, E., 2011, Stratigraphic Architecture of a Net-Transgressive Marginal-to Shallow-Marine Succession: Upper Almond Formation, Rock Springs Uplift, Wyoming, USA: Journal of Sedimentary Research, v. 81, p. 513-533.

Kirschbaum, M., and Hettinger, R., 1998, Stratigraphy and depositional environments of the late Campanian coal-bearing Neslen/Mount Garfield formations, Eastern Book Cliffs, Utah and Colorado:US Geological Survey report number 98-43.

Kirschbaum, M.A., and Hettinger, R.D., 2004, Facies Analysis and Sequence Stratigraphic Framework of Upper Campanian Strata (Neslen and Mount Garfield Formations, Bluecastle Tongue of the Castlegate Sandstone, and Mancos Shale), Eastern Book Cliffs, Colorado and Utah: U.S. Geological Survey Digital Data Series, U.S. Geological Survey, 1 sheet.

Kirshbaum, M.A., and Spear, B.D., 2012, Stratigraphic cross section of measured sections and drill holes of the Neslen Formation and adjacent formations, Book Cliffs Area, Colorado and Utah: US Geological Survey open field report 2012-1260.

Kosters, E.C., and Bailey, A., 1983, Characteristics of peat deposits in the Mississippi River delta plain: Gulf Coast Association of Geological Societies Transactions, v. 33, p.311-325.

Lavigne, J.M., 1999, Aspects of marginal marine sedimentology, stratigraphy and ichnology of the Upper Cretaceous Horseshoe Canyon Formation, Drumheller, Alberta [MSc. Thesis]:, University of Alberta, Edmonton, 146 p.

Lawton, T.F., and Bradford, B.A., 2011, Correlation and Provenance of Upper Cretaceous (Campanian) Fluvial Strata, Utah, U.S.A., from Zircon U-Pb Geochronology and Petrography: Journal of Sedimentary Research, v. 81, p. 495-512.

Leva Lopez, J., Rossi, V., Olariu, C., and Steel, R., 2016, Architecture and recognition criteria of ancient shelf ridges; an example from Campanian Almond Formation in Hanna Basin, USA: Sedimentology, v. XX, p. XX-XX

Longhitano, S.G., Mellere, D., Steel, R.J., and Ainsworth, R.B., 2012, Tidal depositional systems in the rock record: A review and new insights: Sedimentary Geology, v. 279, p. 2-22.

Martinius, A.W., and Gowland, S., 2011, Tide-influenced fluvial bedforms and tidal bore deposits (Late Jurassic Lourinha Formation, Lusitanian Basin, Western Portugal): Sedimentology, v. 58, p. 285-324.

McCabe, P.J., 1985, Depositional Environments of Coal and Coal-Bearing Strata *in* Rahmani, R.A., and Flores, R. M., eds. Sedimentology of Coal and Coal-Bearing Sequences: Blackwell Publishing Ltd: IAS Special Publication v. 7, p. 13-42.

McLaurin, B.T., and Steel, R.J., 2000, Fourth-order nonmarine to marine sequences, middle Castlegate Formation, Book Cliffs, Utah: Geology, v. 28, p. 359-362.

Mellett C.L., Hodgson, D.M., Lang, A., Mauz, B., Selby, I., and Plater, A.J., 2012, Preservation of a drowned gravel barrier complex: A landscape evolution study from the north-eastern English Channel: Marine Geology, v. 315–318, p. 115-131.

Miall, A.D., 1993, The architecture of fluvial-deltaic sequences in the Upper Mesaverde Group (Upper Cretaceous), Book Cliffs, Utah: Geological Society, London, Special Publications, v. 75, p. 305-332.

Miall, A.D., 1996, The geology of fluvial deposits, Springer, Berlin, 582 p.

Miall, A.D., and Arush, M., 2001, The Castlegate Sandstone of the Book Cliffs, Utah: Sequence Stratigraphy, Paleogeography, and Tectonic Controls: Journal of Sedimentary Research, v. 71, p. 537-548.

Miall, A.D., Catuneanu, O., Vakarelov, B.K., and Post, R., 2008, The Western Interior Basin, *in* Andrew, D.M., ed., Sedimentary Basins of the World, Chapter 9, Elsevier, p. 329-362.

Miller, R., Fram, M., Fujii, R. and Wheeler, G., 2008, Subsidence Reversal in a Re-established Wetland in the Sacramento-San Joaquin Delta, California, USA. San Francisco: Estuary and Watershed Science, v. 6, p. 1-20.

Mjos, R., Walderhaug, O. and Prestholm, E. 2009, Crevasse splay sandstone geometries in the Middle Jurassic Ravenscar Group of Yorkshire, UK. Alluvial Sedimentation, International Association of Sedimentologists, Special Publications, v. 17, p. 167-184.

Muto, T., and Steel, R.J., 2001, Autostepping during the transgressive growth of deltas: Results from flume experiments: Geology, v. 29, p. 771-774.

Muto, T., and Steel, R.J., 2002, Role of autoretreat and A/S changes in the understanding of deltaic shoreline trajectory: a semi-quantitative approach: Basin Research, v. 14, p. 303-318.

Muto, T., Steel, R.J., and Swenson, J.B., 2007, Autostratigraphy: a framework norm for genetic stratigraphy: Journal of Sedimentary Research, v. 77, p. 2-12.

Nadon, G.C., 1998, Magnitude and timing of peat-to-coal compaction: Geology, v. 26, p. 727-730.

Nyberg, B., and Howell, J. A., 2016, Global distribution of modern shallow marine shorelines. Implications for exploration and reservoir analogue studies: Marine and Petroleum Geology, v. 71, p. 83-104.

O'Byrne, C.J., and Flint, S., 1995, Sequence, parasequence, and intraparasequence architecture of the Grassy Member, Blackhawk Formation, Book Cliffs, Utah, USA, *in* Van Wagoner J.C., and Bertram G.T., eds., Sequence Stratigraphy of Foreland Basin Deposits, v. 64, p. 225-255.

Olariu, C., Steel, R.J., Olariu, M.I., and Choi, K.S., 2015, Facies and architecture of unusual fluvial-tidal channels with inclined heterolithic strata: Campanian Neslen Formation, Utah, USA, *in* Ashworth, P.J., Best, J.L., and Parsons, D.R., eds., Fluvial-Tidal Sedimentology: Developments in Sedimentology 68, p.353-394.

Olariu, M.I., and Olariu, C., 2015, Ubiquity of Wave-Dominated Deltas In Outer-Shelf Growth-Faulted Compartments. Journal of Sedimentary Research, v.85, p. 768-779.

Olsen, T., Steel, R., Hogseth, K., Skar, T., and Roe, S.L., 1995, Sequential architecture in a fluvial succession; sequence stratigraphy in the Upper Cretaceous Mesaverde Group, Prince Canyon, Utah: Journal of Sedimentary Research, v. 65, p. 265-280.

Orton, G., and Reading, H., 1993, Variability of deltaic processes in terms of sediment supply, with particular emphasis on grain size: Sedimentology, v. 40, p. 475-512.

Penland, S., Boyd., and Suter, J.R., 1988, Transgressive depositional systems of the Mississippi delta plain: a model for barrier shoreline and shelf sand development: Journal of Sedimentary Research, v. 58, p. 932-949.

Pitman, J.K., Franczyk, K.J., and Anders, D.E., 1986, Marine and Nonmarine gas-bearing rocks in Upper Cretaceous Neslen and Blackhawk foramtions, Eastern Uinta Basin, Utah-Sedimentology, Diagenesis, and Source rock potential: AAPG Bulletin, v. 71, p. 76-94.

Posamentier, H.W., and Allen, G.P., 1993, Variability of the sequence stratigraphic model: effects of local basin factors: Sedimentary Geology, v. 86, p. 91-109.

Richards, K., Chandra, S., and Friend, P., 1993, Avulsive channel systems: characteristics and examples: Geological Society, London, Special Publications, v. 75, p. 195-203.

Rittersbacher, A., Howell, J.A., and Buckley, S.J., 2014, Analysis of Fluvial Architecture in the Blackhawk Formation, Wasatch Plateau, Utah, U.S.A., Using Large 3D Photorealistic Models: Journal of Sedimentary Research, v. 84, p. 72-87.

Robinson Roberts, L.N.R., and Kirschbaum, M.A., 1995, Paleogeography and the Late Cretaceous of the Western Interior of middle North America; coal distribution and sediment accumulation, U. S. Geological Survey Professional Paper 1561, 115 p.

RUDOLPH, K.W., DEVLIN, W.J., and CRABAUGH, J.P., 2015, Upper Cretaceous Sequence Stratigraphy of the Rock Springs Uplift, Wyoming: The Mountain Geologist, v. 52, p. 13-157.

RYER, T.A., and LANGER, A.W., 1980, Thickness change involved in the peat-to-coal transformation for a bituminous coal of Cretaceous age in central Utah: Journal of Sedimentary Research, v. 50. p. 987-992.

RYER, T.A., 1981, Deltaic coals of Ferron Sandstone Member of Mancos Shale: predictive model for Cretaceous coal-bearing strata of Western Interior. AAPG Bulletin,v. 65,p. 2323-2340.

SANDERS, J. E. and KUMAR, N., 1975, Evidence of Shoreface Retreat and In-Place “Drowning” During Holocene Submergence of Barriers, Shelf off Fire Island, New York. Geological Society of America Bulletin, v. 86, p. 65-76.

SCHMIDT, C. W., 2015, Delta Subsidence: An Imminent Threat to Coastal Populations: Environmental Health Perspectives, v. 123, p. 204-209.

SHANLEY, K.W., MCCABE, P.J., and HETTINGER, R.D., 1992, Tidal influence in Cretaceous fluvial strata from Utah, USA: a key to sequence stratigraphic interpretation: Sedimentology, v. 39, p. 905-930.

SHIERS, M.N., MOUNTNEY, N., HODGSON, D.M, and COBAIN, S.L, 2014, Depositional Controls on Tidally Influenced Fluvial Successions, Neslen Formation, Utah, USA: Sedimentary Geology, v. 311, p. 1-16.

SIXSMITH, P.J., HAMPSON, G. J., GUPTA, S., JOHNSON, H. D. and FOFANA, J.F., 2008, Facies architecture of a net transgressive sandstone reservoir analog: The Cretaceous Hosta Tongue, New Mexico. AAPG Bulletin, v. 92, p. 513-547.

SPEARS, D.A., 1987, Mineral matter in coals, with special reference to the Pennine coal fields, *in:* Scott, A.C. ed., Coal and coal bearing strata: Recent advances. Geological Society of London Special Publication, v. 32, p. 171-185.

STEEL, R.J., PLINK-BJORKLUND, P. and ASCHOFF, J., 2012, Tidal Deposits of the Campanian Western Interior Seaway, Wyoming, Utah and Colorado, USA, *in*: Davis, R.W., and Dalrymple, R.W., eds., Principles of Tidal Sedimentology: Berlin, Springer, p. 437-471.

STOUTHAMER, E., CHOHEN, K. and GOUW, M.J., 2011, Avulsion and its implications for fluvial-deltaic architecture: insights from the Holocene Rhine-Meuse Delta, *in:* Davidson S.K., Leleu S., North C.P. eds., From River to Rock Record: The Preservation of Fluvial Sediments and Their Subsequent Interpretation, SEPM Special Publication,v. 97, p. 215-232.

SYVITSKI, J.P.M., and FARROW, G.E., 1983, Structures and processes in bayhead deltas: Knight and Bute inlet, British Columbia: Sedimentary Geology, v. 36, p. 217-244.

TABET, D. E., QUICK, J. C., and HUCKA, B. P., 2008, Distribution, Amount, and Maturity of Coal Resources of Most of the Sego Coalfield, Utah, in Longman, M.W., and Morgan C.D., eds. Rocky Mountain Association of Geologists and Utah Geological Association Publication, v. 37, p. 339-365.

TAYLOR, A.M., and GOLDRING, R., 1993, Description and analysis of bioturbation and ichnofabric: Journal of the Geological Society, v. 150, p. 141-148.

TAYLOR, K.G., and MACHENT, P.G., 2011, Extensive carbonate cementation of fluvial sandstones: An integrated outcrop and petrographic analysis from the Upper Cretaceous, Book Cliffs, Utah: Marine and Petroleum Geology, v. 28, p. 1461-1474.

THOMAS, R.G., SMITH, D.G., WOOD, J.M., VISSER, J., CALVERLEYRANGE, E.A., and KOSTER, E.H., 1987, Inclined heterolithic stratification-terminology, description, interpretation and significance: Sedimentary Geology, v. 53, p. 123-179.

TONKIN, N.S., 2012, Deltas, *in* Knaust, D and Bromley, R.G., Trace fossils as indicators of sedimentary environments: Developments in Sedimentology 64, Elsevier, p. 507-528.

TORNQVIST, T.E., WALLACE, D.J., STORMS, J.E., WALLINGA, J., VAN DAM, R.L., BLAAUW, M., DERKSEN, M.S., KLERKS, C.J., MEIJNEKEN, C. and SNUDERS, E.M., 2008, Mississippi Delta subsidence primarily caused by compaction of Holocene strata: Nature Geoscience, v. 1, p. 173-176.

VALASEK, D., 1995, The Tocito Sandstone in a sequence stratigraphic framework: An example of landward-stepping small-scale genetic sequences, in J. C. Van Wagoner and G. T. Bertram,

eds., Sequence stratigraphy of foreland basin deposits: Outcrop and subsurface examples from the Cretaceous of North America: AAPG Memoir 64, p. 349– 369.
van Asselen, S., Stouthamer, E., and van Asch, T.W.J., 2009, Effects of peat compaction on delta evolution: A review on processes, responses, measuring and modeling: Earth-Science Reviews, v. 92, p. 35-51.
Willis, A., 2000, Tectonic control of nested sequence architecture in the Sego Sandstone, Neslen Formation and upper Castlegate Sandstone (Upper Cretaceous), Sevier foreland basin, Utah, USA: Sedimentary Geology, v. 136, p. 277-317.
Willis, B.J., and Gabel, S., 2001, Sharp-based, tide-dominated deltas of the Sego Sandstone, Book Cliffs, Utah, USA: Sedimentology, v. 48, p. 479-506.
Willis, B.J., and Gabel, S.L., 2003, Formation of Deep Incisions into Tide-Dominated River Deltas: Implications for the Stratigraphy of the Sego Sandstone, Book Cliffs, Utah, U.S.A: Journal of Sedimentary Research, v. 73, p. 246-263.
Yoshida, S., 2000, Sequence and facies architecture of the upper Blackhawk Formation and the Lower Castlegate Sandstone (Upper Cretaceous), Book Cliffs, Utah, USA: Sedimentary Geology, v. 136, p. 239-276.
Yoshida, S., Willis, A., and Miall, A.D., 1996, Tectonic control of nested sequence architecture in the Castlegate Sandstone (Upper Cretaceous), Book Cliffs, Utah: Journal of Sedimentary Research, v. 66, p. 737-748.
Young, R.G., 1955, Sedimentary facies and intertonguing in the Upper Cretaceous of the Book Cliffs, Utah- Colorado: Geological Society of America Bulletin, v. 66, p. 177-202.
Young, R.G., 1957, Late Cretaceous cyclic deposits, Book Cliffs, Eastern Utah: Bulletin of the American Association of Petroleum Geologists, v. 41, p. 1790-1774.

CAPTIONS

Table 1 Table describing the geometry, facies and ichnology of representative architectural elements of the lower Neslen Formation. Each element is interpreted in terms of representative sub-environments.

Fig. 1. (A) Conceptual model of a hypothetical fluvial dominated coastline subject to the action of varying processes and showing the likely morphology (modified after Ainsworth et al. 2010); the likely position of the Neslen Formation is indicated in the outlined box. (B) Graph (Y-Y’) showing the hypothetical process variability laterally along the fluvial dominated coastline. (C) Graph (X-X’) showing the variation of processes through the fluvial to marine transition zone. Modified in part after Dalrymple and Choi (2007).

Fig. 2. Sequence Stratigraphic framework of the Book Cliffs, from Tusher Canyon (west) to Lipan Wash (CO) (Line of section is shown in Fig. 4). The panel is based upon works by Kirschbaum and Hettinger (2004); Kirschbaum and Spear (2012) and Shiers et al. (2014); and

has necessitated grouping of depositional environments in order to integrate multiple interpretations. Marker beds (Kirschbaum and Spear 2012; Shiers et al. 2014) are indicated including the Sulphur Canyon Sandstone Bed (SCSB), Thompson Canyon Sandstone Bed (TCSB) and Basal Ballard Sandstone Bed (BBSB). Sequence boundaries and flooding surfaces are numbered in ascending order. Locations for this study are indicated in red, location names are shown on Fig. 4.

Fig. 3. (A) Stratigraphy of the Mesaverde Group in the Book Cliffs between Price (UT) and Grand Hogback (CO) modified after Kirschbaum and Hettinger 2004. (B) Informal stratigraphic subdivision of the Neslen Formation (cf. Shiers et al. 2014) within the study area. Zones within the formation are highlighted and a schematic representation of the stacking of sand bodies (yellow), coal (black) and floodplain fines (gray) is indicated. Sequence boundaries and flooding surfaces are indicated on Figure 2. TCSB – Thompson Canyon Sandstone Bed, BBSB – Basal Ballard Sandstone Bed. SB stands for Sequence Boundary, TS is Transgressive Surface and MFS is Maximum Flooding Surface, numbered surfaces refer to the surfaces in Figure 2.

Fig. 4. Location maps of the study area. (A) Map illustrating the position of the study area along the Book Cliffs (modified after Taylor and Machent 2011). (B) Location of each study locality projected onto a west-east transect; (WF = West Floy Canyon; EF = East Floy Canyon; WM = West Crescent Mine; CC = Crescent Canyon; RHC = Right Hand Crescent Canyon; EC = East Crescent Canyon; WB = West Blaze Canyon; BC = Blaze Canyon; WT = West Thompson Canyon; ES = East Sego Canyon; SW = Salt Wash; ESW = East Salt Wash; SC = Sagers Canyon). Each study locality is composed of measured vertical profiles (Fig. 5) and stratigraphic panels. Line of transect is indicated by the orange line, and is shown on Figs. 5, 8.

Fig. 5. Sedimentary logs recorded at each study locality, detailing the facies and ichnology alongside the interpreted architectural elements. Logs are hung from the base of the

Thompson Canyon Sandstone Bed which acts as a marker for the succession. Refer to Figure 2 for study locations.

Fig. 6 Representative photographs of sedimentary facies and ichnology observed within the Neslen Formation. (A) Wavy and flaser bedding within a bay-fill sandstone element (S_6), draped asymmetrical ripples are visible in the lower part of the photograph. (S_5). (B) Silt-draped asymmetric ripples within a sandstone dominated point bar element (S_2). (C) Sandstone exhibiting cross-bedding with multiple reactivation surfaces within a distributary channel element (S_1). (D) *Thalassinoides* observed at the base of the lower TCSB (S_5). (E) *Teredolites* bored wood found in the base of a heterolithic point bar element (S_3). (F) Highly bioturbated sandstone of the TCSB (S_5); Thompson Canyon Sandstone Bed; examples of *Ophiomorpha* are common; bioturbation index of 3 (Taylor and Goldring 1993)

Fig. 7 Representative architectural elements of the Neslen Formation; description and interpretation of elements can be found in Table 1. (A) Distributary channel-fill element (S_1). (B) Sandstone-prone lateral accretion element (S_2). (C) Isolated heterolithic lateral accretion element (S_3). (D) Amalgamated inclined heterolithic stratification (S_4). (E) Tabular reworked shoreface sandstone element (S_5). (F) Bay-fill sandstone element (S_6). (G) Stacked overbank sandstone elements (F_1). (H) Repeated arrangements of fining-upwards floodplain elements (F_2). (I) Coal-prone floodplain elements (F_3), interbedded with examples of overbank sandstone and fining-upwards floodplain elements.

Fig. 8 Correlation panel of the logged sections located along the line of section (to scale) (Figure 4). Interpreted packages (see text) are indicated as are marker units: Basal Ballard Sandstone Bed and Thompson Canyon Sandstone Bed. Shaded grey regions represent coal-bed correlations.

Fig. 9 Summary of vertical trends through the lower Neslen Formation. An idealized, composite sedimentary section is shown on the left-hand side and is divided into the interpreted depositional packages. Regressive intervals (green) and transgressive intervals (blue) are indicated the line of section along with the position of interpreted flooding surfaces. (A) Architectural element proportions (for key see Figure 7). (B) Summary paleocurrent orientations for each package; orange represents bedding or lateral accretion surfaces, blue represents the dip direction of ripples and cross-bedded strata. (C) Occurrence of key indicators of marine (tidal and wave indicators) and brackish water conditions. Sedimentary indicators (dark blue) are interpreted to represent fluctuations in current energy and directions. Marine to brackish ichnogenera includes *Ophiomorpha, Arenicolites, Thalassinoides Rhizocorallium, Bergaueria,* and *Diplocraterion*. (D) Paleogeographic reconstruction for each package; accurate in the proportion and dimensions of architectural elements and paleoflows. Circles represent study sites. See Figure 5 for key.

Fig. 10 (A) Modified sea-level curve for the lower Neslen Formation; sequence boundaries and flooding surfaces are named on Figure 2. Depositional packages are as follows: Lower Palisade Zone (LPZ), Palisade Coal Zone (PCZ), Middle Palisade Zone (MPZ), Upper Palisade Zone (UPZ), Basal Ballard Sandstone Bed (BBSB), Ballard Coal Zone (BCZ) and Thompson Canyon Sandstone Bed (upper and lower) (TCSB). Intervals of regression (R; green) and transgression (T; blue) are indicated along the sea-level curve. (B) Schematic architecture of the decompacted lower Neslen Formation. (C) Relationship of the lower Neslen Formation within the broader sequence stratigraphic panel (Fig. 2). Key for architectural elements is shown in Figure 5.

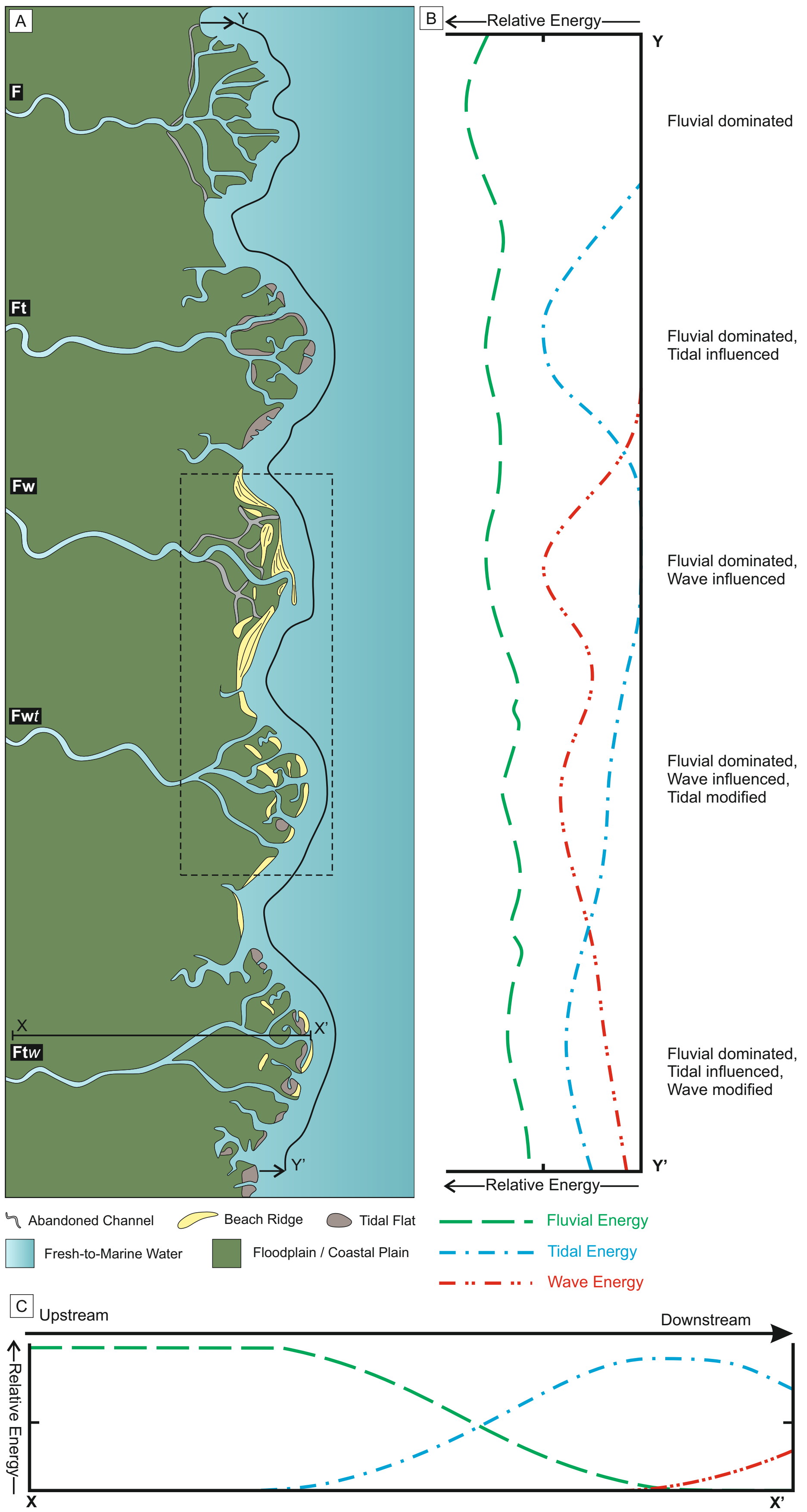

A
Y
F
Ft
Fw
Fwt
X
X'
Ftw
Y'
B
Relative Energy
Y
Fluvial dominated
Fluvial dominated, Tidal influenced
Fluvial dominated, Wave influenced
Fluvial dominated, Wave influenced, Tidal modified
Fluvial dominated, Tidal influenced, Wave modified
Y'
Relative Energy
Abandoned Channel
Beach Ridge
Tidal Flat
Fresh-to-Marine Water
Floodplain / Coastal Plain
Fluvial Energy
Tidal Energy
Wave Energy
C
Upstream
Downstream
Relative Energy
X
X'

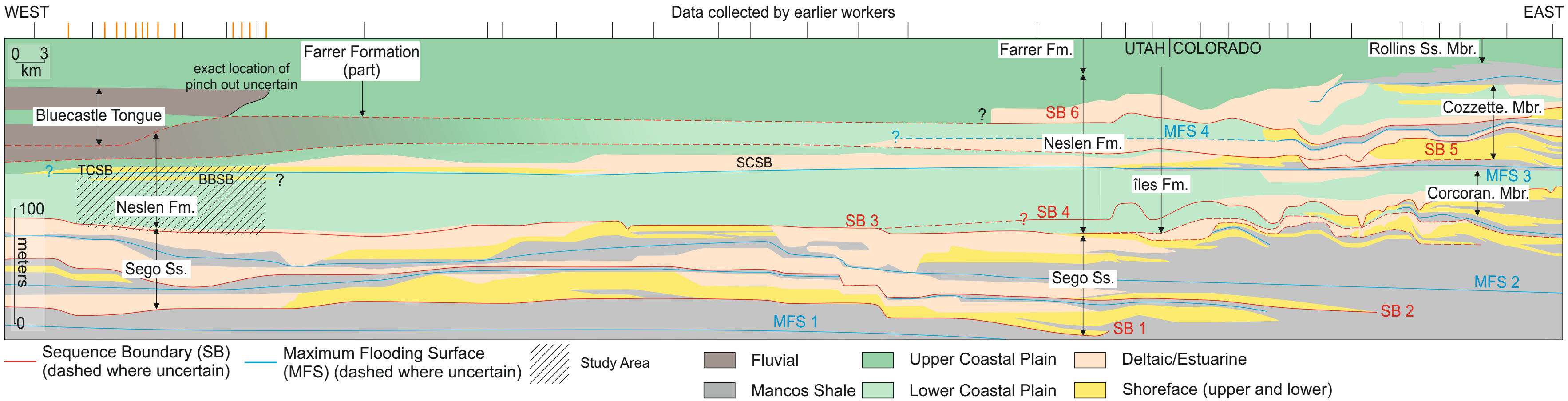

WEST
Data collected by earlier workers
EAST
0 3 km
Bluecastle Tongue
exact location of pinch out uncertain
Farrer Formation (part)
Farrer Fm.
UTAH
COLORADO
Rollins Ss. Mbr.
Cozzette. Mbr.
SB 6
MFS 4
Neslen Fm.
SB 5
MFS 3
TCSB
BBSB
SCSB
Neslen Fm.
îles Fm.
Corcoran. Mbr.
100
SB 3
SB 4
meters
Sego Ss.
Sego Ss.
MFS 2
SB 2
0
MFS 1
SB 1
Sequence Boundary (SB) (dashed where uncertain)
Maximum Flooding Surface (MFS) (dashed where uncertain)
Study Area
Fluvial
Mancos Shale
Upper Coastal Plain
Lower Coastal Plain
Deltaic/Estuarine
Shoreface (upper and lower)

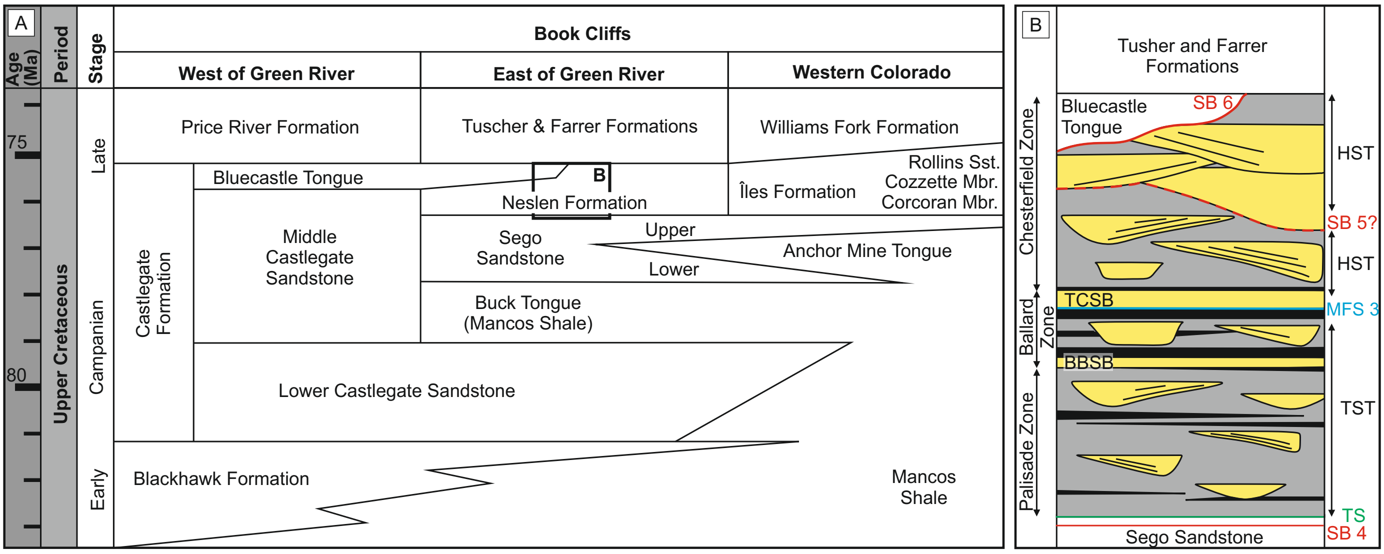

A
Age (Ma)
Period
Stage
Book Cliffs
West of Green River
East of Green River
Western Colorado
75
80
Upper Cretaceous
Late
Campanian
Early
Price River Formation
Tuscher & Farrer Formations
Williams Fork Formation
Bluecastle Tongue
B
Neslen Formation
Rollins Sst.
Cozzette Mbr.
Corcoran Mbr.
Îles Formation
Castlegate Formation
Middle Castlegate Sandstone
Sego Sandstone
Upper
Lower
Anchor Mine Tongue
Buck Tongue (Mancos Shale)
Lower Castlegate Sandstone
Blackhawk Formation
Mancos Shale
B
Tusher and Farrer Formations
Bluecastle Tongue
SB 6
HST
SB 5?
HST
TCSB
MFS 3
BBSB
TST
TS
SB 4
Sego Sandstone
Chesterfield Zone
Ballard Zone
Palisade Zone

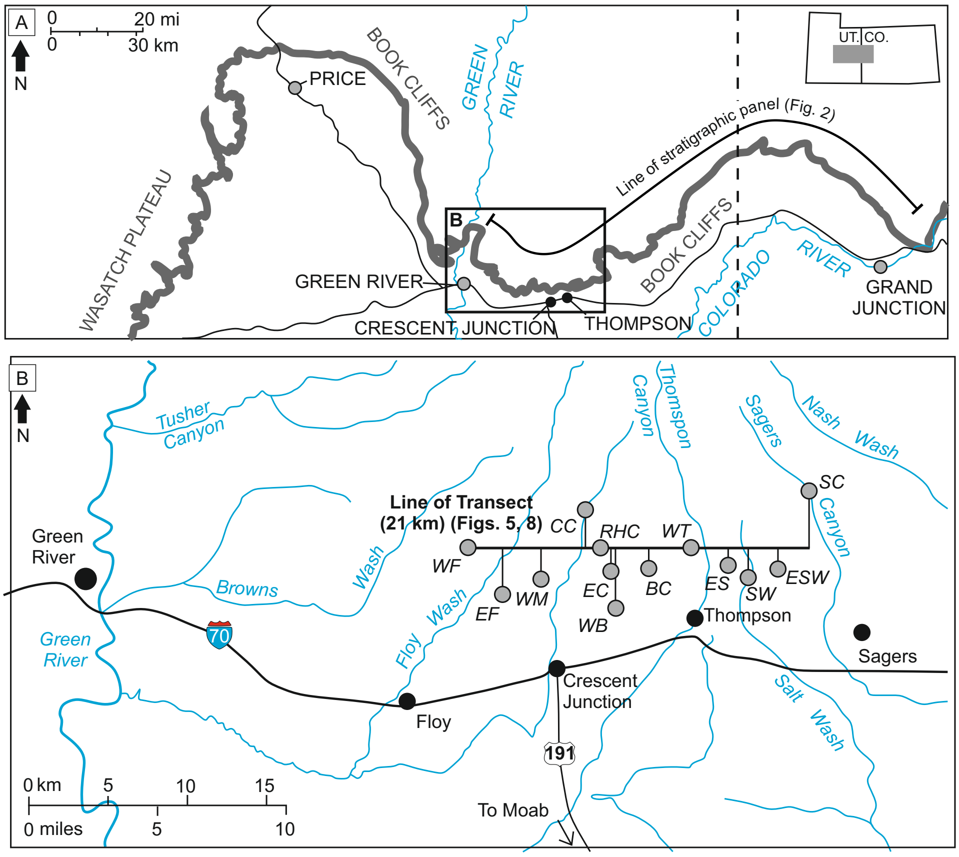
A
0
20 mi
0
30 km
N
PRICE
BOOK CLIFFS
GREEN RIVER
WASATCH PLATEAU
UT.
CO.
Line of stratigraphic panel (Fig. 2)
B
GREEN RIVER
CRESCENT JUNCTION
THOMPSON
BOOK CLIFFS
COLORADO
RIVER
GRAND JUNCTION
B
N
Tusher Canyon
Browns
Wash
Green River
Green River
Line of Transect (21 km) (Figs. 5, 8)
CC
RHC
WT
WF
EF
WM
EC
WB
BC
ES
SW
ESW
SC
Canyon
Thompson
Sagers
Nash Wash
Canyon
Floy Wash
70
Thompson
Sagers
Crescent Junction
Floy
191
Salt Wash
0 km
5
10
15
0 miles
5
10
To Moab

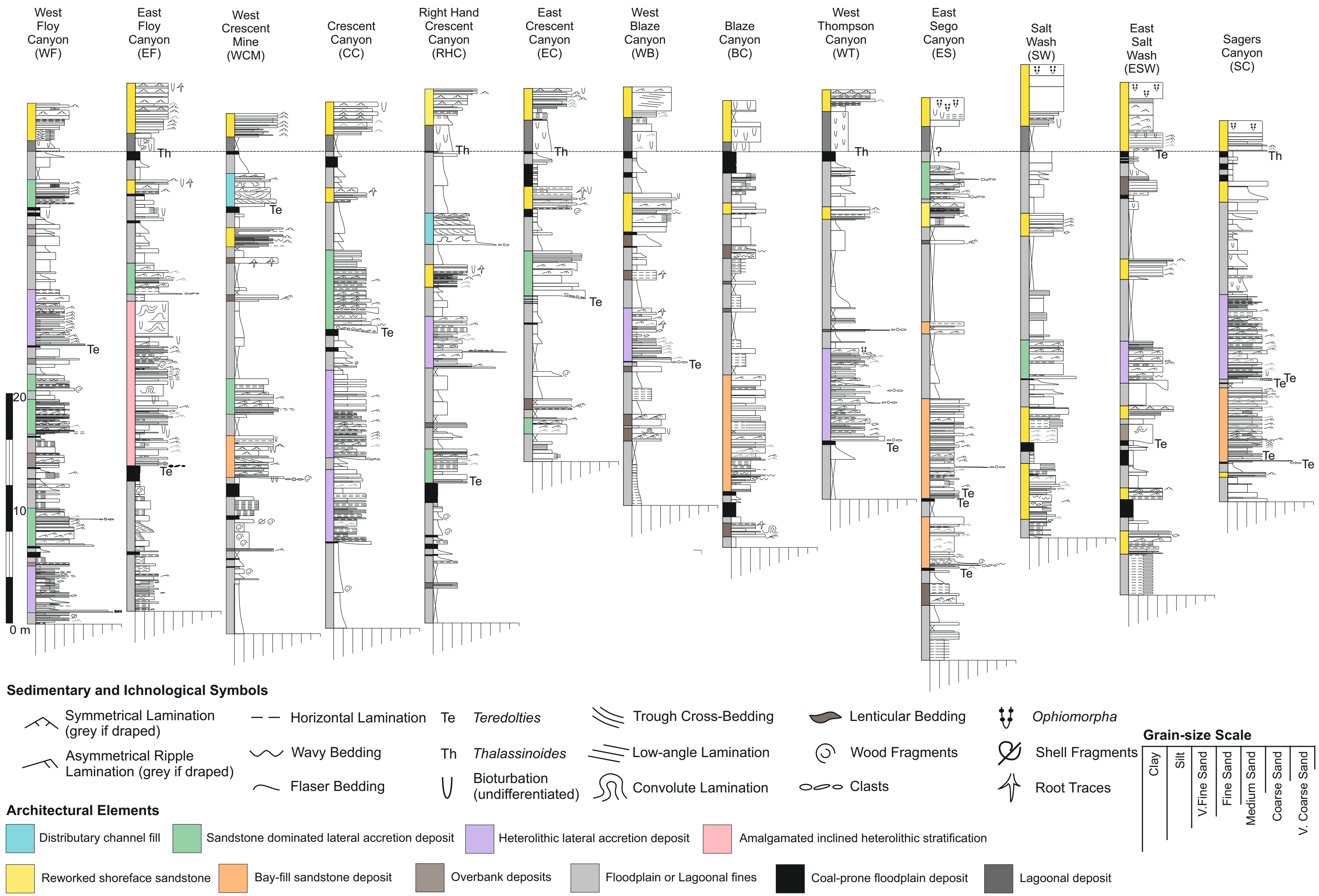

West Floy Canyon (WF)
East Floy Canyon (EF)
West Crescent Mine (WCM)
Crescent Canyon (CC)
Right Hand Crescent Canyon (RHC)
East Crescent Canyon (EC)
West Blaze Canyon (WB)
Blaze Canyon (BC)
West Thompson Canyon (WT)
East Sego Canyon (ES)
Salt Wash (SW)
East Salt Wash (ESW)
Sagers Canyon (SC)
20
10
0 m
Th
Te
?
Sedimentary and Ichnological Symbols
Symmetrical Lamination (grey if draped)
Asymmetrical Ripple Lamination (grey if draped)
Horizontal Lamination
Wavy Bedding
Flaser Bedding
Te Teredolties
Th Thalassinoides
Bioturbation (undifferentiated)
Trough Cross-Bedding
Low-angle Lamination
Convolute Lamination
Lenticular Bedding
Wood Fragments
Clasts
Ophiomorpha
Shell Fragments
Root Traces
Grain-size Scale
Clay
Silt
V.Fine Sand
Fine Sand
Medium Sand
Coarse Sand
V. Coarse Sand
Architectural Elements
Distributary channel fill
Sandstone dominated lateral accretion deposit
Heterolithic lateral accretion deposit
Amalgamated inclined heterolithic stratification
Reworked shoreface sandstone
Bay-fill sandstone deposit
Overbank deposits
Floodplain or Lagoonal fines
Coal-prone floodplain deposit
Lagoonal deposit

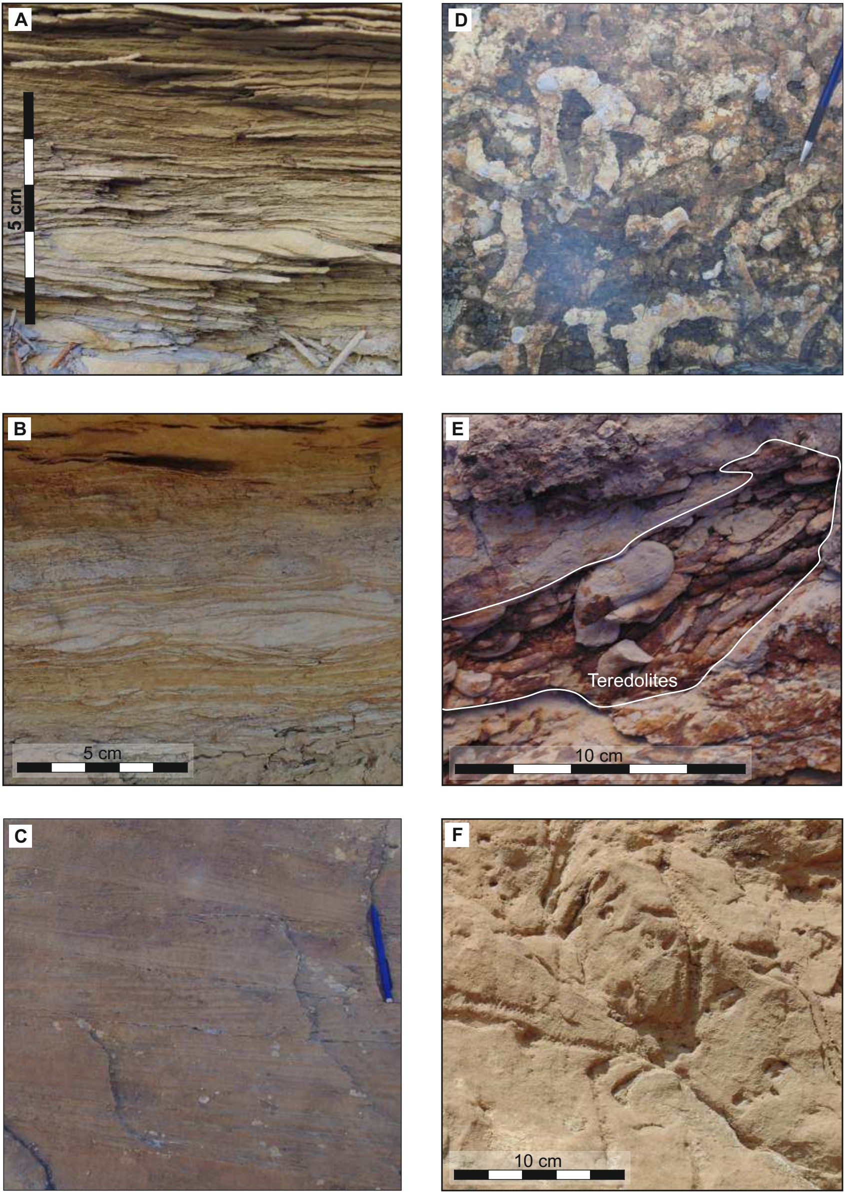

A
5 cm
D
B
5 cm
E
Teredolites
10 cm
C
F
10 cm

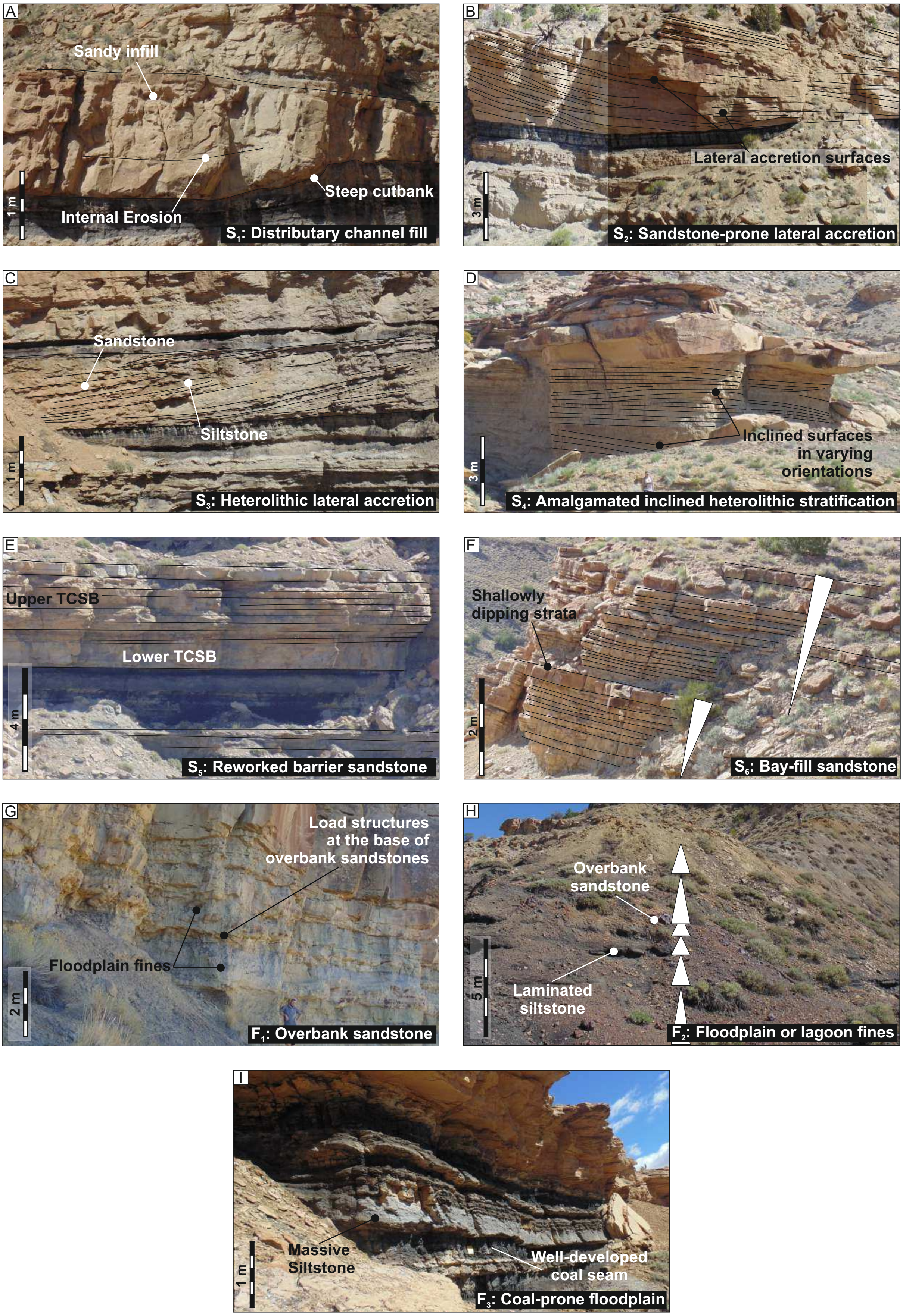
A
Sandy infill
Internal Erosion
Steep cutbank
1 m
S1: Distributary channel fill
B
Lateral accretion surfaces
3 m
S2: Sandstone-prone lateral accretion
C
Sandstone
Siltstone
1 m
S3: Heterolithic lateral accretion
D
Inclined surfaces
in varying
orientations
3 m
S4: Amalgamated inclined heterolithic stratification
E
Upper TCSB
Lower TCSB
4 m
S5: Reworked barrier sandstone
F
Shallowly
dipping strata
2 m
S6: Bay-fill sandstone
G
Load structures
at the base of
overbank sandstones
Floodplain fines
2 m
F1: Overbank sandstone
H
Overbank
sandstone
Laminated
siltstone
5 m
F2: Floodplain or lagoon fines
I
Massive
Siltstone
Well-developed
coal seam
1 m
F3: Coal-prone floodplain

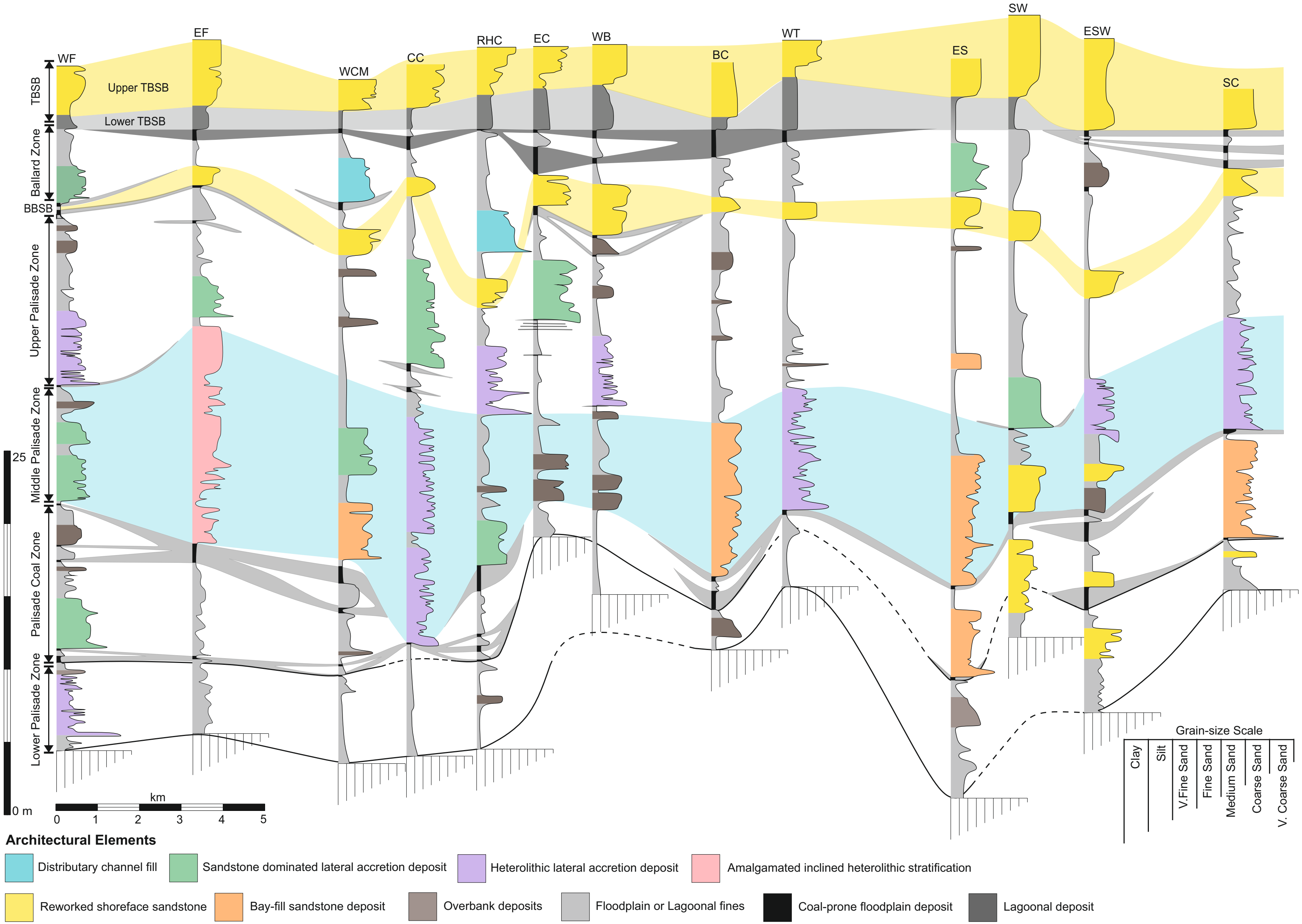

WF
EF
WCM
CC
RHC
EC
WB
BC
WT
ES
SW
ESW
SC
TBSB
Upper TBSB
Lower TBSB
Ballard Zone
BBSB
Upper Palisade Zone
Middle Palisade Zone
Palisade Coal Zone
Lower Palisade Zone
25
0 m
km
0 1 2 3 4 5
Grain-size Scale
Clay
Silt
V.Fine Sand
Fine Sand
Medium Sand
Coarse Sand
V. Coarse Sand
Architectural Elements
Distributary channel fill
Sandstone dominated lateral accretion deposit
Heterolithic lateral accretion deposit
Amalgamated inclined heterolithic stratification
Reworked shoreface sandstone
Bay-fill sandstone deposit
Overbank deposits
Floodplain or Lagoonal fines
Coal-prone floodplain deposit
Lagoonal deposit

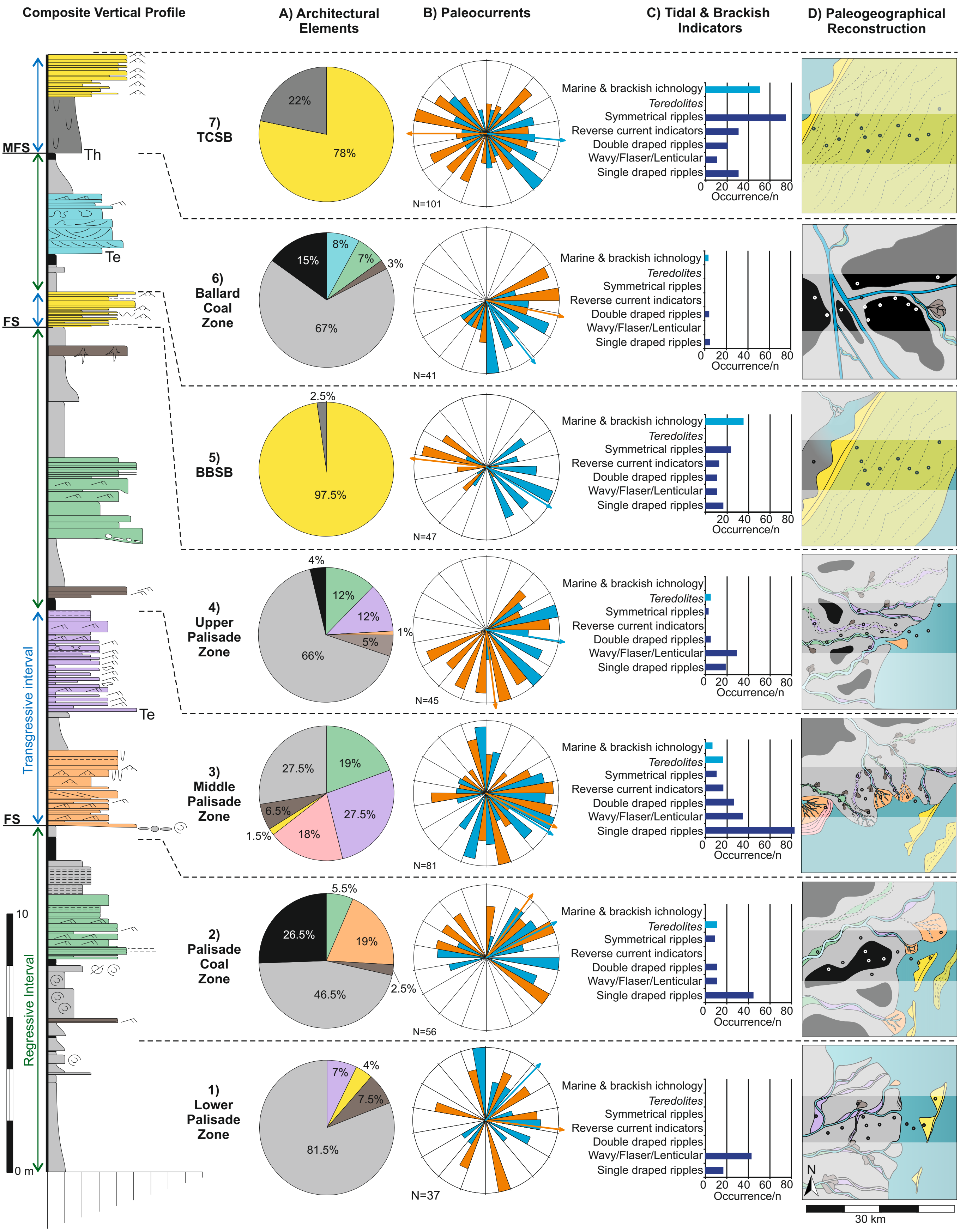

Composite Vertical Profile
A) Architectural Elements
B) Paleocurrents
C) Tidal & Brackish Indicators
D) Paleogeographical Reconstruction
MFS
FS
FS
Th
Te
Te
Transgressive interval
Regressive Interval
10
0 m
7) TCSB
22%
78%
N=101
6) Ballard Coal Zone
8%
7%
3%
15%
67%
N=41
5) BBSB
2.5%
97.5%
N=47
4) Upper Palisade Zone
4%
12%
12%
1%
5%
66%
N=45
3) Middle Palisade Zone
27.5%
19%
6.5%
27.5%
1.5%
18%
N=81
2) Palisade Coal Zone
5.5%
26.5%
19%
2.5%
46.5%
N=56
1) Lower Palisade Zone
7%
4%
7.5%
81.5%
N=37
Marine & brackish ichnology
Teredolites
Symmetrical ripples
Reverse current indicators
Double draped ripples
Wavy/Flaser/Lenticular
Single draped ripples
0 20 40 60 80
Occurrence/n
N
30 km

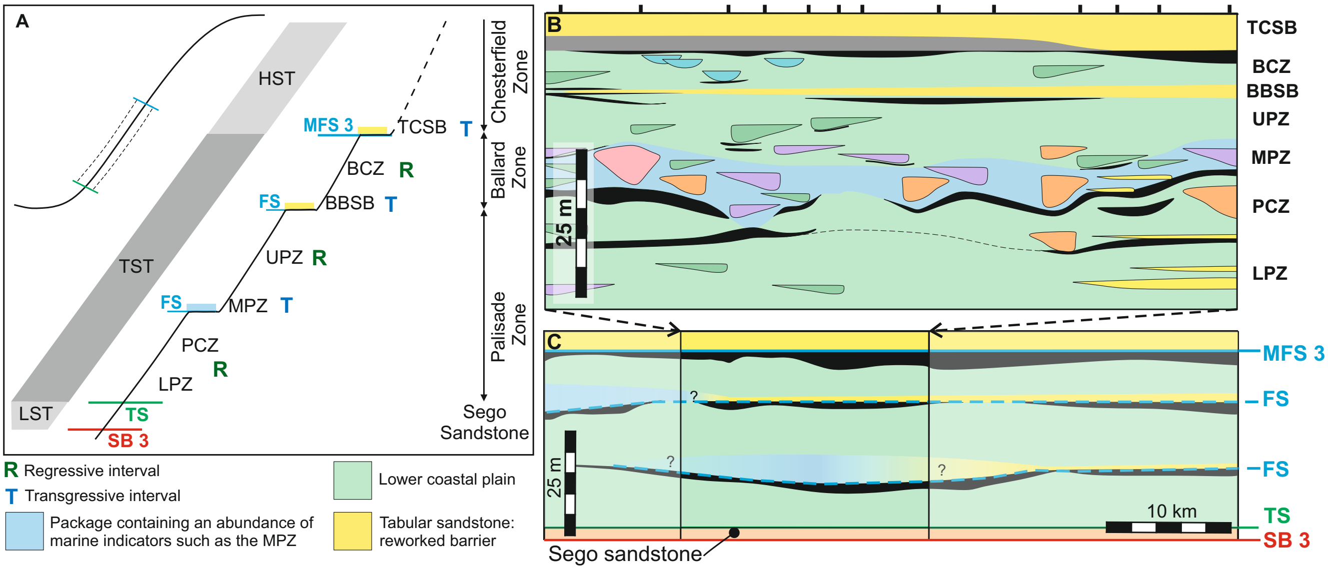
A
HST
TST
LST
MFS 3
TCSB
T
BCZ
R
FS
BBSB
T
UPZ
R
FS
MPZ
T
PCZ
R
LPZ
TS
SB 3
Chesterfield Zone
Ballard Zone
Palisade Zone
Sego Sandstone
R Regressive interval
T Transgressive interval
Package containing an abundance of marine indicators such as the MPZ
Lower coastal plain
Tabular sandstone: reworked barrier
B
TCSB
BCZ
BBSB
UPZ
MPZ
PCZ
LPZ
25 m
C
MFS 3
FS
FS
TS
SB 3
25 m
10 km
Sego sandstone
?
?
?

Architectural element	Geometry and dimensions	Description	Ichnology	Relationship to other elements	Interpretation
S_1- Distributary channel-fill	Abrupt pinchouts with steep cut-banks (35°). Basal incision 4-7 m which is equal to the element thickness. Width 35-200 m and low aspect ratio of 10-15.	Aggradational fine- to medium-sandstone arranged into sets separated by erosion surfaces. Scour surfaces overlain by intraformational conglomerate. Cross bedding is common towards the base, passing upwards into ripple cross-laminated sandstone. Sigmoidal co-sets; convex-up cross bedding are recognized. Drapes of siltstone and carbonaceous material occur. No Lateral accretion surfaces are observed.	BI 1; examples of *Skolithos* and *Arenicolites* towards the base of the element.	Erosionally overlie elements F_1, F_2 and F_3.	Distributary channels (Miall 1996), unidirectional flow with migrating, large-scale dunes and minor modification by tidal currents (drapes on foresets) in a backwater environment (cf. Colombera et al. 2016)
S_2- Sandstone-prone lateral accretion	Commonly exhibit a lenticular form with thicknesses of 2-6 m and with basal incision up to 3 m deep. Width of 90-500 m. Inclined surfaces dip at 6-20°.	Fining upwards from fine-grained to very fine-grained sandstone. Lenticular beds (5-40 cm) downlap onto lower beds or the basal surface. Lithofacies include massive-to-faintly laminated sandstone with ripples, climbing ripple cross-lamination and cross-bedding.	BI 1-2 in beds at the top of element.	Erosionally overlie elements F_1, F_2 and F_3.	Channelized unidirectional flow with a high degree of levee confinement. Dominance of lateral accretion typical of fluvial point bars (cf. Bridge, 2006).
S_3- Isolated heterolithic lateral accretion	Thicknesses up to 5 m and 50-300 m wide. Bed surfaces dip at 5-25°.	Alternating tabular- to wedge–shaped beds of well-sorted, fine-grained sandstone and siltstone. Sandstone beds (0.05-1 m thick) display ripple cross-lamination, horizontal lamination and low-angle cross-lamination. Single and double drapes on ripple foresets are common. Rare occurrences of opposing dip directions in ripple foresets. Siltstone beds (5-10 cm thick) exhibit lenticular-flaser-wavy laminations.	BI 0-3 (higher in upper parts of element) including *Arenicolites*, *Diplocraterion*, *Rhizocorallium*. *Teredolites* is common at the base.	Commonly pass laterally and erosionally overlie elements F_1, F_2 and F_3.	Inclined surfaces represent lateral accretion in heterolithic point bars (Inclined Heterolithic Stratification; Thomas et al. 1987). Presence of brackish water ichnofacies, draped ripples and current reversals indicate marine influence on these deposits (Shanley et al., 1992).

Architectural element	Geometry and dimensions	Description	Ichnology	Relationship to other elements	Interpretation
S_4-Amalgamated IHS	Beds are horizontal or inclined up to 8° within elements that are up to 16 m thick. Within each element, packages attain a maximum thickness of 4 m and can be traced laterally for up to 150 m.	Stacked heterolithic bed-sets of alternating sandstone, siltstone and mudstone. Overall the beds within each package thicken and coarsen upwards. Sandstone beds are massive to laminated and exhibit ripples with single- and double-drapes of mud and carbonaceous material. Finer- grained beds are generally laminated to massive but in places also exhibit flaser, lenticular and wavy bedding.	BI 0-3 with *Medousichnus*, *Planolites* and *Palaeophycus*. Gastropod (*Viviparus*) and bivalve fragments with *Teredolites* at the base.	Commonly overlies elements F_1-F_3. Lateral relationships are typically poorly exposed.	Inclined clinoforms at varying angles on a small scale indicate a small-scale prograding delta (crevasse delta, Gilbert-type delta or bay-head delta) in a sheltered marine environment (Syvitski and Farrow 1983; Joeckel and Korus 2012). A fluvial interpretation is rejected based upon the ichnology and the thickening and coarsening upwards trend within each package.
$_5$-Reworked Barrier Sandstone	Thickness varies from 1-6 m (for the sandy upper part). The finer lower part (where present) is 1-1.5 m thick. Lateral extent is 100s m to 10s of km. In some areas, shallowly dipping (up to 7°) clinoforms dipping to the west are observed. Beds are tabular, wedging out over 100s of meters.	Examples of this element occur in, but are not exclusive to, the TCSB and BBSB. The finer-grained lower part of this element is only observed in examples in the TCSB and is composed of heavily bioturbated dark grey siltstone and very fine-grained sandstone containing shell fragments and siderite bands. The sandy upper part is observed in all examples and comprises thickening- and coarsening-up packages of clean, well sorted sandstone. Where not obscured by bioturbation, beds are 50-150 mm thick and exhibit symmetrical ripple-lamination (mud draped in lower beds), and horizontal lamination.	Lower TCSB – heavily bioturbated (BI 5) overprinting of original sedimentary structures. *Thalassinoides* abundant on the base. Upper TCSB and other examples: BI 0-5 increases both upwards down-dip. Bioturbation includes *Arenicolites*, *Bergueria* *Planolites* and *Ophiomorpha*. Crawling and root traces on top surfaces.	Commonly underlain and overlain by thick, well developed coal (F_3) or by floodplain or lagoonal fines (F_2). Lateral transitions at the point of pinch out are not directly observed.	The lower division represents a lagoonal setting, subject to intense bioturbation. Sedimentary structures and ichnology in the upper part represent a brackish water, wave dominated environment e.g. washover fans, shoreface, or a sand-spit (Kirschbaum and Hettinger 2004). A retreating barrier bar interpretation is favored based on the geometry and scale of the elements (Penland et al. 1988). A bay-fill is discounted due to the down-dip extent of the bodies and the lack of erosional surface.

Architectural element	Geometry and dimensions	Description	Ichnology	Relationship to other elements	Interpretation
S_6- Bay-fill sandstone	Elements up to 5 m thick and 20-100 m in lateral extent. Erosion at the base of the element is up to 30 cm. Bed boundaries become increasingly erosive upwards.	Thickening- and coarsening-upwards from very fine- to fine-grained sandstone characterized by horizontal and ripple laminations, commonly with single or double drapes (mud, silt or carbonaceous). Interbedded sandstone and siltstone beds exhibit load casts and convolute lamination and lenticular, flaser and wavy bedding. Intraformational conglomerate occurs on internal scour surfaces.	BI 0-3 including *Ophiomorpha*, *Rhizocorallium* and *Diplocraterion.* Root traces towards the top.	Commonly overlies elements F_1-F_3. Lateral relationships are typically poorly exposed	Tide and wave influence, brackish water ichnology and shallowing upwards succession indicates environments such as crevasse deltas or mouth-bars (Joeckel and Korus, 2012).
F_1- Overbank sandstone	Elements are less than 2 m thick and pinch out gradually over tens to hundreds of meters. Localized erosion up to 30 cm at the base.	Very fine- to fine-grained sandstone and siltstone. Beds dip in varying orientations at low angles (2-5°). Weathering and the occurrence of post-depositional concretions obscure sedimentary structures. Lithofacies include massive sandstone, climbing and current ripple and horizontal laminations	BI 0. Rare root casts are preserved.	Passes laterally and vertically into element F_2; commonly overlies element F_1.	Un-confined flows on levees, crevasse channel and splays. Incision indicates slightly higher energy flows (Guion et al., 1995; Mjos et al. 2009).
F_2- Floodplain and lagoonal fines	Packages are up to 5 m thick and have a lateral extent of tens to hundreds of meters.	Brown to black mudstone and siltstone arranged into fining upwards packages. A: Common sulfur staining, wood fragments, coalified wood debris and rooted horizons. B: Passes vertically from laminated siltstone to massive mudstone, notably absent of rooted horizons, deformed (flattened) coal and amber clasts.	A: BI 0. Occasional root casts are preserved. B: BI 0-3 Some bioturbation of indeterminable origin.	A: Overlain by coals of element F_3, commonly grades upwards from F_1. B: Commonly overlain or underlain by elements S_4-S_6.	A: Accumulation in low-energy settings such as distal crevasse splays (Guion et al., 1995). B: Accumulation in quiet water brackish settings such as lagoons (Horne et al., 1978). The two sub-elements are not always readily discernible and association with other elements must be considered.
F_3- Coal-prone floodplain	Various scales are preserved from mm-sized ribbons to meter-thick beds of tens to hundreds of meters lateral extent.	Black, friable coals containing amber and wood fragments, as well as sandstone clasts. Coals do not occur as simple sheets but interfinger with clastic facies.	Lenses of sand can represent sandy infill of burrows.	Commonly occur at the top of element F_2 and are commonly overlain by sandier elements (F_1, S_2-S_7)	Coals formed in raised peat mires in humid, swampy conditions (Davies et al., 2006; Jerrett et al., 2011a).